MULTIPION PRODUCTION IN DIFFRACTIVE HADRONIC REACTIONS

by

Richard Gagnon

A thesis submitted to the Faculty of Graduate Studies and Research of McGill University, in partial fulfilment of the requirements for the degree of Doctor of Philosophy.

Department of Physics
McGill University

Montreal, Quebec
August 1978

SOMMAIRE

Un modèle hybride est présenté dans lequel une "fireball", particule fortement excitée, formée de manière dynamique se désintègre en cascade selon le modèle du "bootstrap" statistique. Cette "fireball" est constituée d'un ensemble très dense de résonances. Les lois de conservation de l'isospin et de la parité G sont pleinement satisfaites et il est tenu compte de la largeur finie des résonances produites. La densité totale des états de la "fireball" est calculée et le modèle est utilisé pour le calcul des distributions de masse et des sections efficaces relatives dans les diffusions diffractives pion-proton et pion-deutéron. L'accord entre la théorie et les données expérimentales disponibles est en général très bon. Diverses prédictions pour les événements à haute multiplicité sont faites. La conclusion générale est que le modèle donne une description satisfaisante de la production de trois pions dans le secteur de Lorentz avant (LPS#1) alors qu'il s'avère très approprié pour décrire les phénomènes diffractifs à haute multiplicité.

ABSTRACT

We present a hybrid model in which a fireball seen as a dense set of overlapping resonances is dynamically formed and subsequently decays in cascade according to the statistical bootstrap model. Full account is taken of isospin and G-parity conservations as well as of the finite widths of the produced resonances. This model allows an explicit calculation of the total density of states in a fireball. It is applied to diffractive pion dissociation on nucleon and nuclear targets for which multipion mass distributions and relative cross-sections are calculated. Agreement with available experimental data is in general very good. Several predictions for high multiplicity are given. The general conclusion is that the model gives a satisfactory description of the three-pion events in the forward LPS sector and is very well suited to describe higher multiplicity diffractive phenomena.

A mes parents, M. et Mme. Louis-Philippe Gagnon

et à mon épouse, Louise.

ACKNOWLEDGMENTS

I would like to take this opportunity to thank all people who to different extents made the realization of this thesis possible. I thank all graduate students in the theoretical high energy group for many stimulating discussions, in particular, my friend Michel Létourneau. Thank you to Paul Antaki for his stylistic help in carrying out the manuscript and to Martine Banville for her restless effort in typing it. I am grateful to Charles Lessard and Richard Turcotte for their beautiful work in making drawings and graphs. I also thank Dr. Claude Leroy for a careful reading of this thesis.

Finally, but not the least, I would like to acknowledge the invaluable help of my advisor, Professor B. Margolis, for his competent guidance throughout this work.

TABLE OF CONTENTS

		Page
	SOMMAIRE	ii
	ABSTRACT	iii
	ACKNOWLEDGMENTS	v
	TABLE OF CONTENTS	vi
I	INTRODUCTION	1
II	A MODEL FOR DIFFRACTIVE MULTIPION PRODUCTION	5
	II-1 General Considerations	5
	II-2 The Formation of a Fireball	8
	II-3 Statistical Bootstrap Model	15
	II-4 Average Multiplicities and Decay Scheme	18
III	TOTAL DENSITY OF STATES AND APPLICATION TO PION-PROTON SCATTERING	22
	III-1 Introduction	22
	III-2 Dynamical Formation of a Fireball	22
	III-3 Linear Statistical Bootstrap Model	27
	III-4 Calculation of the Density of States	30
	III-4-A The Resulting Density of States	37
	III-5 Multipion Production in Pion-Proton Scattering	39
	III-5-A Production of Three Pions	43
	III-5-B Production of Five Pions	45

III-5-C Seven and Nine-Pion Production 47

III-5-D Relative Cross-Sections 48

III-6 Non-Linear Statistical Bootstrap Model 49

III-6-A Effect of the Non-Linear Contribution on Multipion Production 53

IV APPLICATION TO PION-DEUTERON SCATTERING 56

IV-1 Introduction 56

IV-2 Coherent Production on Nuclei 57

IV-3 Multipion Production in Pion-Deuteron Scattering 59

IV-4 Relative Cross-Sections 62

V SUMMARY AND CONCLUSIONS 65

APPENDIX I : Initial Conditions in the Linear Bootstrap (Density of States) 71

APPENDIX II : Initial Conditions in the Linear Bootstrap (Exclusive Channels) 87

APPENDIX III : Initial Conditions in the Non-Linear Bootstrap (Exclusive Channels) 91

APPENDIX IV : Three-Body Phase-Space 96

REFERENCES 99

TABLES (2) 103

FIGURE CAPTIONS 105

FIGURES (11) 108

CHAPTER I

INTRODUCTION

Quite naturally, statistical models appeared in high energy physics when the number of particles being produced in a reaction started to increase. The idea was that in this kind of process dynamical considerations would average out due to the great number of different components interfering with each other. Equally naturally, the concept of cluster or fireball emerged, in analogy to the compound nucleus in nuclear physics or the statistical model of Fermi [1.1]. A number of models based on this idea were formulated such as the thermodynamical model of Hagedorn and Ranft [1.2] in which a continuum of fireballs is produced or the one of Elvekjaer and Steiner [1.3] in which the same cluster is used to describe hadron-hadron, photon-hadron and e^+e^- processes or a recent one attempting to apply information theory to multiparticle physics developed by Carazza, Ernst, Gandolfi and Schmitt [1.4].

In this thesis, we shall concentrate our attention to diffractive dissociation processes and present a model in which a fireball is dynamically formed through Regge exchange in the t-channel and then decays statistically in the s-channel. Though we shall apply it to exclusive processes, this is the spirit of the double fireball model of Hwa [1.5] or the statistical model of Ranft and Ranft [1.6] for inclusive reactions.

Many features characterize diffraction dissociation phenomena [1.7]. For instance, the strong forward peak in the differential cross-sections and the slow energy dependence of the integrated cross-section. Experiments performed at 200GeV on pp [1.8] and $\pi^- p$ [1.9] scattering show that the diffractive low multiplicity states have the same behavior as observed at lower energies. This is not surprising once we realize that diffraction is highly peripheral and thus a change in the incident momentum should have little effect. Peripherality also explains why no intrinsic quantum numbers are exchanged in these reactions except of course spin and parity since there can be angular momentum transfer. However, it is found empirically that the transfer of angular momentum between the two colliding particles is minimal thus allowing the production of states of the unnatural parity sequence $(0^-, 1^+, 2^-, \ldots)$. This result is embodied in the so-called Gribov-Morrison rule:

$$P_f = P_i (-1)^{\Delta j} \qquad (I.1)$$

where P_i and P_f are respectively the parity of the initial and final systems and Δj the change of spin. It seems however that this rule is not general since some A_2 production has been reported recently in diffractive pion dissociation [1.10].

Many particles have been seen to dissociate diffractively: pion, kaon, nucleon and even Σ^- [1.11] on either nucleon or nuclear targets. The mass distribution of the disso-

ciating system shows an enhancement in the low-mass range above the threshold associated with the production of two-body states. For instance, the A_1 and A_3 peak near the threshold of $\rho\pi$ and $f\pi$ production respectively. But this tendency may not persist and in fact, in the model we shall present [1.12], higher multiplicity spectra are not dominated by two-body states but rather are the results of a summation over many different contributions obtained in a fireball decay cascade.

The idea is the following: in diffractive dissociation, as we said before, the produced particles form a system having the same intrinsic quantum numbers (except spin and parity) as those of the hadron being dissociated. This suggests that they might come from a cluster or fireball being produced through pomeron exchange. As we shall show, it consists of a statistically dense set of overlapping resonances whose density will be calculated according to the statistical bootstrap model of Hagedorn [1.13] and Frautschi [1.14] and resulting in an exponential increase within powers of M of the number of states. We then make the usual assumption of statistical mechanics: the probability of a particular outcome is given by the ratio of the occupied number of states to the total number of states [1.15]. Most likely, the fireball will decay into two particles, one being as light as possible, the other as heavy as possible [1.14] so that if it is heavy enough, it can be considered in its turn as another fireball. We are thus led

to a cascade decay scheme whose net result is a mass spectrum rapidly increasing at low-mass until the exponential density of states acts as a fast high-mass cut-off [1.16]. No angular momentum considerations are taken into account so that all decays are isotropic in their own rest-frame. This is not a severe restriction since no angular distribution calculations will be attempted. On the other hand, isospin and G-parity conservations are fully taken into account. Finite widths of discrete resonances produced in the reaction are also incorporated leading to a good description of threshold phenomena and to a general smoothing of the mass distributions.

This thesis is divided into five chapters. In chapter II, the general formalism of the model is developed. It is shown how the formation of a dense set of resonances results in fireball production. A brief description of the statistical bootstrap model is also given. Chapter III deals with the calculation of the total density of states, of multipion mass distributions and of relative cross-sections in pion-proton scattering. In chapter IV, similar calculations are done on a deuterium target. A summary and conclusions of this thesis are presented in chapter V. In order not to break continuity of the text, we have collected in four appendices initial conditions of equations to be evaluated as well as a derivation of the general non-invariant three-body phase-space.

CHAPTER II

A MODEL FOR DIFFRACTIVE MULTIPION PRODUCTION

II-1 General Considerations.

To produce multipion states, we shall construct a two-component model describing independently the formation of a fireball and its subsequent decay. Consider for instance the process

$$a + b \to n\pi + c \qquad \text{(II.1.1)}$$

where a,b and c are stable particles under strong interactions. Our model states that this reaction proceeds in two stages as follows:

$$a + b \to \sum_i R_i + c \qquad \text{(II.1.2)}$$
$$R_i \to n\pi$$

Here, the R_is are all possible resonances which have a non-zero branching ratio into the $(n\pi)$ channel. Each of them is characterized by its mass M_i and its width Γ_i. They are formed during the first-stage of the reaction which is then seen as a quasi two-body reaction. This formation mechanism is dynamical in nature and therefore depends on the particular reaction considered. Since we are mainly interested here in multipion

enhancements diffractively produced, we shall consider essentially that a pomeron exchange gives rise to these highly excited resonances. It is to be noticed that in such a case, each resonance will retain the intrinsic quantum numbers of particle a, except for spin and parity. We leave a more detailed study of this first stage to chapters where applications are considered.

The second stage of the reaction deals with the decay of the resonances. We shall assume no final state interaction between their decay products and particle c. This amounts to assuming that resonances are sufficiently long-lived (their width is sufficiently narrow) that their decay is completely independent of what happened previously and in particular of the way they have been formed. In the next section, we shall show that if these resonances are close enough to each other (which will happen as the mass of the resonances increases) one can replace reaction (II.1.2) by

$$a + b \to \underbrace{F}_{n\pi} + c \qquad \text{(II.1.3)}$$

where F is a superposition of overlapping resonances which we call a fireball. This is depicted diagrammatically in figure 2.1.

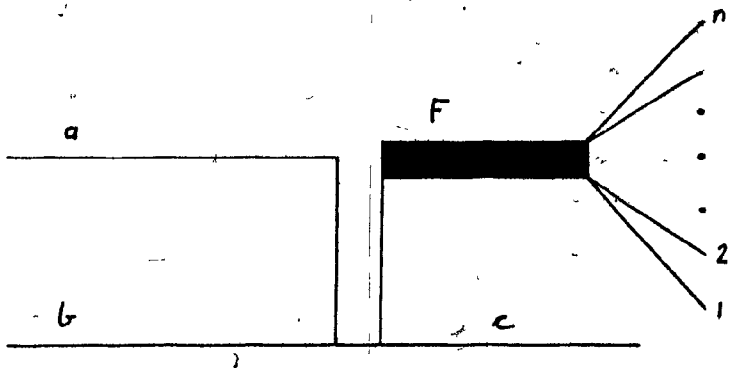

Figure 2.1: Regge exchange giving rise to a fireball which then decays into n-pion states.

II-2 The Formation of a Fireball.

We shall now establish the formalism in which the fireball is formed. In order to do so, we have to calculate the cross-section for the diagram of figure 2.2. We start with the cross-section for the process (II.1.1) which in general is given by:

$$\sigma = \frac{1}{2\lambda^{\frac{1}{2}}(s,m_a^2,m_b^2)} \frac{1}{(2\pi)^{3n-1}} \frac{1}{n!} \int d^4p_c \prod_{i=1}^{n} d^4q_i \delta(p_c^2-m_c^2)$$

$$\times \delta(q_i^2-m_i^2)\, \delta^4(p_a+p_b-p_c-\Sigma q_i)\, |T(a+b\to n\pi+c)|^2 \qquad (II.2.1)$$

where s is the square of the total center-of-mass energy, m_a, m_b and p_a, p_b are respectively the masses and the four-momenta of the incoming particles, m_c and the m_i's, p_c and the q_i's are respectively the masses and the four-momenta of the outgoing particles. In our case, all m_i's are equal to m_π, the pion mass. 1/n! is the statistical factor for n identical pions in the final state and

$$\lambda(x,y,z) \equiv x^2 + y^2 + z^2 - 2xy - 2xz - 2yz \qquad (II.2.2)$$

We next introduce a unity factor:

$$1 = \int d^4Q \delta^4(Q-\Sigma q_i) \qquad (II.2.3)$$

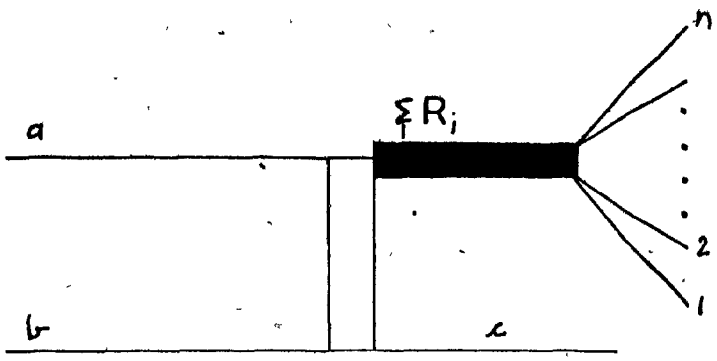

Figure 2.2: Formation of a set of resonances decaying into n-pions.

where Q will represent the four-momentum of the n-pion system. We factorize the amplitude into the form appropriate for reaction (II.1.2).

$$T(a + b \to n\pi + c) = \sum_k T(a + b \to R_k + c) \frac{1}{(M_k^2 - M^2) - iM_k\Gamma_k} \times T(R_k \to n\pi) \qquad \text{(II.2.4)}$$

where $T(a + b \to R_k + c)$ is the production amplitude of resonance R_k, $T(R_k \to n\pi)$ its decay amplitude into n pions and $1/\left[(M_k^2 - M^2) - iM_k\Gamma_k\right]$ is the resonance propagator or its effective mass distribution. M_k and Γ_k are respectively the mass and total width of the resonance. We have also summed over all possible resonances which can decay into n pions.

Inserting (II.2.3) and (II.2.4) into (II.2.1), one has:

$$\sigma = \frac{1}{2\lambda^{\frac{1}{2}}(s, m_a^2, m_b^2)} \frac{(n!)^{-1}}{(2\pi)^{3n-1}} \int d^4p_c d^4Q \prod_{i=1}^{n} d^4q_i \delta(p_c^2 - m_c^2) \times \delta(q_i^2 - m_\pi^2) \delta^4(Q - \sum_i q_i) \delta^4(p_a + p_b + p_c - Q) \times \sum_{k,l} \frac{T^*(a + b \to R_k + c) T^*(R_k \to n\pi)}{(M_k^2 - M^2) + iM_k\Gamma_k} \cdot \frac{T(a + b \to R_l + c) T(R_l \to n\pi)}{(M_l^2 - M^2) + iM_l\Gamma_l} \qquad \text{(II.2.5)}$$

We shall now assume a high degree of randomness or a rapid oscillation of the relative signs of the phase of the different production and decay amplitudes. This leads to a dominance of the incoherent k = 1 terms. The off-diagonal terms, to the extent that they do not cancel, would give a component slowly varying with energy typical of Regge behavior (I.16). Then, the cross-section reduces to:

$$\sigma \simeq \sum_k \frac{1}{2\lambda^{\frac{1}{2}}(s,m_a^2,m_b^2)} \frac{(n!)^{-1}}{(2\pi)^{3n-1}} \int d^4p_c\, d^4Q\, \delta(p_c^2-m_c^2)$$

$$\times\, \delta^4(p_a + p_b - p_c - Q)\ |T(a+b \to R_k + c)|^2$$

$$\times\, \frac{1}{\left[(M_k^2 - M^2)^2 + M_k^2\Gamma_k^2\right]} \int d^4q_i\, \delta(q_i^2 - m_\pi^2)$$

$$\times\, \delta^4(Q - \sum_i q_i)\ |T(R_k \to n\pi)|^2 \qquad \text{(II.2.6)}$$

and since

$$\Gamma(R_k \to n\pi) = \frac{1}{2M_k} \frac{1}{(2\pi)^{3n-4}} \frac{1}{n!} \int \prod_{i=1}^{n} d^4q_i\, \delta(q_i^2 - m_\pi^2)$$

$$\times\, \delta^4(Q - \sum_i q_i)\ |T(R_k \to n\pi)|^2 \qquad \text{(II.2.7)}$$

where $\Gamma(R_k \to n\pi)$ is the partial width of resonance R_k to decay into n pions, we obtain:

$$\sigma = \sum_k \frac{1}{2\lambda^{\frac{1}{2}}(s,m_a^2,m_b^2)} \frac{1}{(2\pi)^2} \int d^4p_c d^4Q \delta(p_c^2 - m_c^2) \cdot$$

$$\times \delta^4(p_a + p_b - p_c - Q) \cdot |T(a + b \to R_k + c)|^2$$

$$\times \frac{1}{\left[(M_k^2 - M^2)^2 + M_k^2\Gamma_k^2\right]} \frac{M_k}{\pi} \Gamma(R_k \to n\pi) \qquad \text{(II.2.8)}$$

So far, all matrix elements are exact, but from here on, we shall neglect angular momentum and spin effects. Therefore, conservation of angular momentum will not be taken into account. We do not expect this to be a too severe restriction (1.1,2.1) and to have big effects on the results, except of course, for the angular distribution of pions which we shall not attempt to calculate.

As their mass grows, resonances are expected to get closer and closer, becoming, at sufficiently high mass, a continuum of overlapping resonances of density $\rho(M_k)$, enabling us to replace the sum over k by an integral over M_k. This leads to;

$$\sigma \simeq \frac{1}{2\lambda^{\frac{1}{2}}(s,m_a^2,m_b^2)} \frac{1}{(2\pi)^2} \int dM_k \rho(M_k) d^4p_c d^4Q \delta(p_c^2 - m_c^2)$$

$$\times \delta^4(p_a + p_b - p_c - Q) |T(a + b \to R_k + c)|^2$$

$$\times \frac{M_k}{\pi} \frac{\Gamma(R_k \to n\pi)}{\left[(M_k^2 - M^2)^2 + M_k^2\Gamma_k^2\right]} \qquad \text{(II.2.9)}$$

We shall now make the approximation that:

$$\Gamma_k^2/2 << M^2 \qquad \text{(II.2.10)}$$

This is in general true since the width of a typical resonance is of the order of the pion mass while the effective mass of n pions is in the GeV range, already for n=3. In this case, one has:

$$\frac{1}{(M_k^2 - M^2)^2 + M_k^2\Gamma_k^2} \simeq \frac{1}{(M_k^2 - M^2)^2 + M^2\Gamma_k^2} \qquad \text{(II.2.11)}$$

Using Cauchy's theorem to integrate over M_k, we obtain:

$$\sigma \simeq \frac{1}{2\lambda^{\frac{1}{2}}(s,m_a^2,m_b^2)} \frac{1}{(2\pi)^2} \int d^4p_c d^4Q \delta(p_c^2 - m_c^2)$$

$$\times \delta^4(p_a + p_b - p_c - Q) \left|T(a + b \to F + c)\right|^2$$

$$\times \frac{\rho(M)}{M} \frac{\Gamma(F \to n\pi)}{\Gamma(M)} \qquad \text{(II.2.12)}$$

where F denotes a fireball of mass M and of total width $\Gamma(M)$. We see that it consists of a superposition of resonances of density $\rho(M)$.

We now integrate over the fourth component of p_c using

the first delta-fonction and with the help of the second, integrate over Q. In addition, we know that:

$$\frac{d^3p_c}{2E_c} = \frac{dM^2 d\phi_c dt}{4\lambda^{\frac{1}{2}}(s, m_a^2, m_b^2)} \qquad \text{(II.2.13)}$$

The result is:

$$\frac{d\sigma}{dM^2} = \frac{1}{16\pi\lambda(s, m_a^2, m_b^2)} \int dt \left|T(a + b \to F + c)\right|^2 \frac{\rho(M)}{M} \times \frac{\Gamma(F \to n\pi)}{\Gamma(M)} \qquad \text{(II.2.14)}$$

We have assumed rotational invariance with respect to the collision axis to perform the integration over ϕ_c.

Looking at the above derivation, one sees that in fact $|T(a + b \to F + c)|^2$ is the production matrix element of a single resonance of mass M. Instead, we can replace it by the inclusive matrix element for the process:

$$a + b \to c + \text{anything} \qquad \text{(II.2.15)}$$

which corresponds to the production of all resonances in the interval between M and M + dM, provided we divide it by the number of states in this interval, a number proportional to $\rho(M)$.

Therefore, we finally obtain:

$$\frac{d\sigma}{dM^2} = \frac{1}{16\pi\lambda(s,m_a^2,m_b^2)} \int dt\, R(s,t,M)\, \frac{1}{M}\, P(F \to n\pi) \qquad \text{(II.2.16)}$$

where $R(s,t,M)$ is the inclusive matrix element and $P(F \to n\pi)$ is the decay probability of the fireball into n pions as:

$$P(F \to n\pi) = \frac{\Gamma(F \to n\pi)}{\Gamma(M)} \qquad \text{(II.2.17)}$$

This quantity is Lorentz-invariant and hence can be calculated in any frame of reference. For convenience, we shall do the calculation in the rest frame of the fireball.

II-3 Statistical Bootstrap Model.

So far, we have produced one piece of highly excited hadronic matter of mass M: a fireball. This fireball, due to its high mass, can decay into a great number of channels. This suggests that one can average over dynamical effects and utilize a statistical decay scheme. We shall therefore assume, as usual in statistical models (e.g. Fermi model in nuclear physics [1.1]) that the probability of a particular outcome is proportional to the ratio of the number of occupied states to the total number of available states.

Again, here, the states are very dense, and we can

define a density of channels $\rho_{out}(M)$. In addition, each channel can be obtained in many ways and here too, we define a density of states which give rise to the channel $\rho_{in}(M)$. It is clear that for large enough M, $\rho_{in}(M)$ and $\rho_{out}(M)$ will have the same functional dependence since a heavy resonance decays mainly into other resonances which in turn decay into other resonances and so on. So, asymptotically, the spectrum of the "mother" resonance will be the same as the spectrum of the "daughter" resonances. Conversely, one may say that the "daughter" resonances are the constituents of the "mother" resonance. (This explains why the subscripts in and out are used.) Therefore, the density of produced resonances will also be the same.

This is precisely the statistical bootstrap model of Hagedorn [1.13] and Frautschi [1.14]. We shall use here the formulation of Frautschi more suited to particle physics.

One can write the manifestly covariant number of states as [1.14,2.2]

$$\int dM \rho_{out}(M)\ d^4Q 2\omega_\mu Q^\mu \delta(Q^2-M^2)\delta^4(P-Q) = \sum_{n=2}^{\infty} \frac{1}{n!} \prod_{i=1}^{n} \pi$$

$$\times \int dm_i \rho_{in}(m_i) \int d^4q_i 2\omega_{i\mu} q_i^\mu \delta(q_i^2-m_i^2)\delta^4(Q-\sum_{i=1}^{n} q_i)$$

(II.3.1)

where ω_μ is the four-volume of particle i. It is defined as Vu where V is the volume occupied by a particle at rest (which we take universal) and u its four-velocity ($u^2=1$). The

quantity $\omega_\mu q^\mu$ is an invariant equal to $Vq_o/(2\pi)^3$ as easily seen when evaluated in a frame where V is at rest.

The left-hand side of the equation is the number of states that a fireball of mass M can have. The right-hand side is the number of states available to n particles (asymptotically fireballs themselves) constrained by energy-momentum conservation. The sum over n appears because the number of constituents is unfixed and unlimited and the integral over the mass because, in addition to different states of motion, each particle can also be in different states of mass with density $\rho(m_i)$.

In the rest-frame of the fireball, this expression reduces to:

$$\rho_{out}(M) = \sum_{n=2}^{\infty} \left[\frac{V}{(2\pi)^3}\right]^{n-1} \frac{1}{n!} \prod_{i=1}^{n} \int dm_i \rho_{in}(m_i) \int d^3 q_i \times \delta\left(\sum_{i=1}^{n} E_i - M\right) \delta^3\left(\sum_{i=1}^{n} q_i\right) \qquad \text{(II.3.2)}$$

This is the form given by Frautschi. This density is fully covariant as we just saw. In addition, all strong interactions are effectively taken into account since the interaction responsible for the binding of two constituents manifests itself in a change of the density of states [1.14,2.5,2.6]. Therefore, we can treat a fireball as a gas of completely non-interacting particles (repulsive forces are negligible).

It has been shown by Chaichian et al. [2.2] that the above so-called non-covariant phase-space is indeed the right one to use in the case of an ideal gas. The use of the covariant phase-space containing an additional factor m_i/E_i is in fact equivalent to a dynanical assumption which clearly results in favoring low kinetic energies and thus high multiplicities.

An asymptotic analytic solution of equation (II.3.2) can be obtained using the following bootstrap condition:

$$\rho_{in}(M) \xrightarrow[M \to \infty]{} \rho_{out}(M) \qquad \text{(II.3.3)}$$

The resulting density of states is [1.14,2.5,2.6]

$$\rho(M) \xrightarrow[M \to \infty]{} \frac{a e^{M/T}}{M^3} \qquad \text{(II.3.4)}$$

where T can be interpreted as the maximum temperature of hadronic matter [1.13]. T and a (a normalization constant) cannot be calculated but we might expect T to be of the order of the pion mass since above that temperature, pions can be emitted.

II-4 Average Multiplicities and Decay Scheme.

Frautschi calculated also the probability that a fireball is constituted of n objects [1.14]. He found in the high mass limit:

$$P(n) = \frac{(\ln 2)^{n-1}}{(n-1)!} \qquad \text{(II.4.1)}$$

A result independent of the mass of the fireball. This means that a fireball is 69% of the time a two-body object, 24% of the time a three-body object and in only 7% of the cases does it contain more than three bodies. This leads to an average multiplicity $\bar{n}$ of approximately 2.4. Moreover, it turned out that a particular contribution peaks when one particle takes most of the mass of the initial fireball and other particles are light (hence mostly pions). Since our model assumes that a fireball decays according to the relative proportions of its constituents, we are therefore given a decay scheme in which an initial fireball decays predominantly into a pion plus a heavy object which can itself be another fireball if its mass is high enough. In turn, this second fireball is treated as the first one. Occasionally, we shall observe a three-particle decay but rarely four. Thus, we are led to a cascade model of fireball decay as shown in figure 2.3. At each step i of the cascade, we associate a probability of decay into n bodies:

$$P_i(M) = \frac{\rho_n(M)}{\rho(M)} \qquad \text{(II.4.2)}$$

where we denote by $\rho_n(M)$ the n^{th} term contributing to (II.3.2).

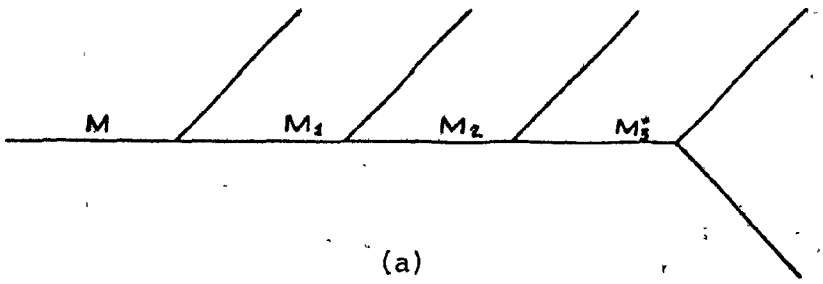

(a)

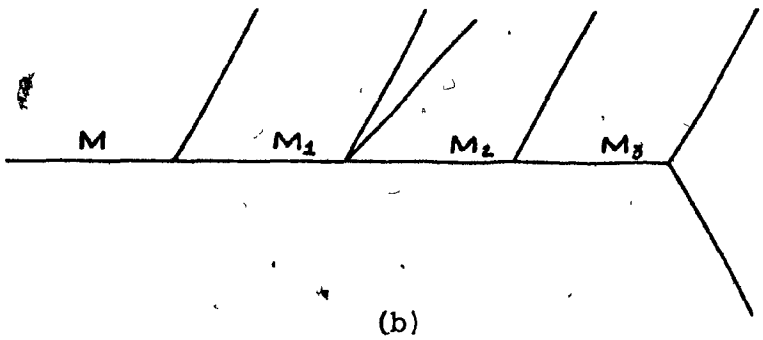

(b)

Figure 2.3 (a) Predominant decay scheme of a fireball in the Frautschi model.

(b) Decay of a fireball exhibiting a three-particle vertex.

The probability of decay of a fireball into n pions (eq.II.2.17) will then be a convolution of expressions like (II.4.2) over the different steps of the cascade.

However, here, we shall not use asymptotic considerations working instead directly with a generalized version of equation (II.3.2) to account for isospin and G-parity conservations, which shall be evaluated numerically.

Clearly, at the end of the chain, even the heavy particle emitted will be rather light and we shall not allow it to become lighter than an ordinary discrete resonance. Even in this case, statistical considerations might not be completely reliable. But this should not be a large source of error especially for long chains which are expected to dominate in any case.

CHAPTER III

APPLICATION TO PION-PROTON SCATTERING

III-1 Introduction.

We are now ready to apply the model developed in chapter II to hadronic reactions. We start with diffractive dissociation in pion-proton scattering at high energy for which we shall calculate the mass spectra of three, five, seven and nine pions as well as the relative production cross-section.

We look at diffractive reactions because it allows us to test the model in a clean way, i.e. we know exactly the quantum numbers of the fireball which are those of the particle being excited (except for spin and parity which we do not take into account); all produced pions come from the same vertex since double diffractive excitation is certainly negligible if it ever exists; finally, the dynamics involved in the fireball formation can safely be handled by keeping it to a minimum since even accounting for all possible contributions to diffraction will not change our results appreciably.

III-2 Dynamical Formation of a Fireball.

We adopted in the previous chapter a formulation of the model in which the mechanism of fireball formation was to be replaced, in this case, by the inclusive cross-section

$$\pi + p \to p + \text{anything} \qquad \text{(III.2.1)}$$

in the fragmentation region of the pion (figure 3.1). At high energies, this process is best described by making a triple-Regge expansion [3.1] as shown in figure 3.2. Several contributions can play a role in this reaction, namely (neglecting interference terms): PPP,PPR,PRR,RRR where P stands for a pomeron and R for a reggeon on a lower trajectory. But it turns out, according to an analysis of Chan Hong-Mo et al. [3.2] that the triple-pomeron term dominates the cross-section for small value of M^2/s (where M is the missing mass). It is clear that a PPR contribution could be added, but as we said before, this would hardly change our results. Thus, for simplicity, only the triple-pomeron term will be kept. Moreover, it seems that these conclusions do not strongly depend on the reaction since a similar analysis of Roy and Roberts [3.3] on proton-proton inclusive reaction in the fragmentation region of a proton led to the same conclusions.

In the triple-Regge formalism, we write the triple-pomeron squared matrix element as (3.4):

$$R(s,t,M) \overset{\sim}{=} \gamma_{PPP}(t) \left(\frac{S}{M^2}\right)^{2\alpha_P(t)} (M^2)^{\alpha_P(0)} \qquad \text{(III.2.2)}$$

where $\gamma_{PPP}(t)$ is the triple-pomeron coupling and $\alpha_p(t)$ is the pomeron trajectory. We shall use the usual linear form:

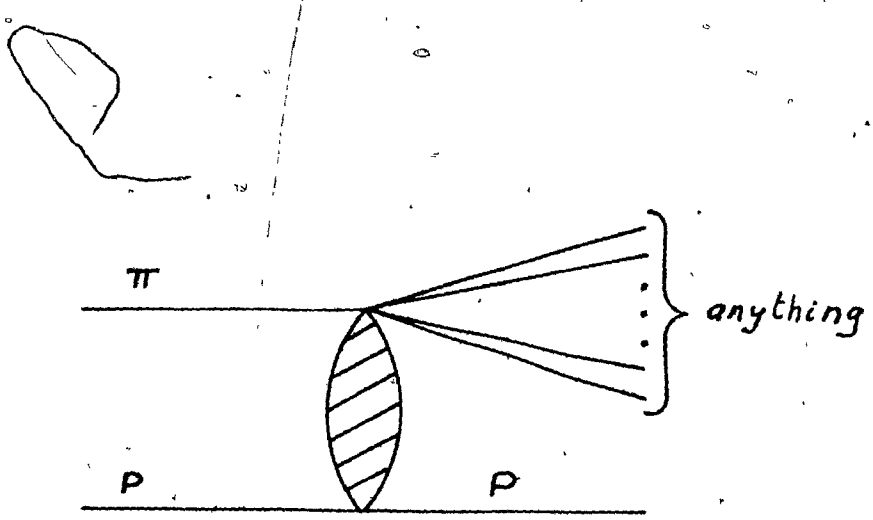

Figure 3.1: Inclusive pion-proton scattering in the fragmentation region.

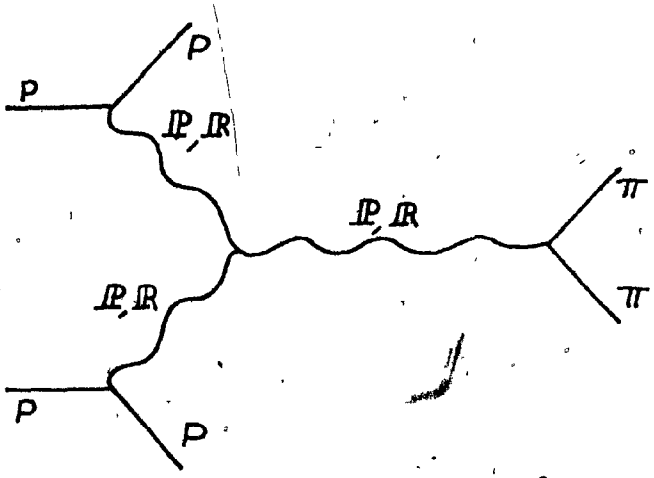

Figure 3.2: Triple-Regge expansion for inclusive reaction at large values of s, M^2, s/M^2 and small fixed t.

$$\alpha_p(t) = 1 + \alpha_p' t \qquad \text{(III.2.3)}$$

Also, following many authors [3.3,3.5], we shall parametrize the coupling constant as:

$$\gamma_{ppp}(t) = a_1 e^{b_1 t} + a_2 e^{b_2 t} \qquad \text{(III.2.4)}$$

Therefore, in pion-proton scattering, the differential cross-section (II.2.16) reads:

$$\frac{d\sigma}{dM^2} \cong \frac{1}{16\pi s^2} \left(\frac{s}{M^2}\right)^2 MP(F\to n\pi) \int_{-\infty}^{0} dt \; (a_1 e^{b_1 t} + a_2 e^{b_2 t}) \times \left(\frac{s}{M^2}\right)^{2\alpha_p' t} \qquad \text{(III.2.5)}$$

where $\lambda(s,m_p^2,m_\pi^2)$ has been replaced by s^2 for large s. The integral is readily done and we find:

$$\frac{d\sigma}{dM^2} = \frac{1}{16\pi} \frac{1}{M^3} \left[\frac{a_1}{b_1+2\alpha_p' \ln(s/M^2)} + \frac{a_2}{b_2+2\alpha_p' \ln\,(s/M^2)}\right] \times P(F \to n\pi) \qquad \text{(III.2.6)}$$

Thus, within logarithms which almost do not vary over the short range of M we shall consider, the cross-section reduces to:

$$\frac{d\sigma}{dM^2} \simeq C \frac{1}{M^3} P(F \to n\pi) \qquad \text{(III.2.7)}$$

where C is a normalization constant. We obtain the same expression we would have obtained by approximating equation (III.2,5) by the cross-section at t=0. This is due to the fact that we are dealing with diffractive scattering which exhibits a very strong peak in the forward direction which accounts for most of the cross-section.

III-3 Linear Statistical Bootstrap Model.

The main contribution to the decay probability comes from the sequential decay of a fireball into a relatively light particle (pion or discrete hadronic resonance) plus another fireball. In a first approximation, we may assume that this two-particle decay accounts for the whole probability. We shall call this version of the model the linear statistical bootstrap.

We shall denote $P_n(M,I,G)$ the probability that a fireball of mass M, of isospin I and of G-parity G decays into n pions. The third component of isospin does not appear as a label since for I<2 (we do not allow for exotic fireballs) it can be shown [3.5] that in a statistical model, the decay is symmetric in isospin space.

Consider for instance the process:

$$F(M) \rightarrow F_1(m_1) + P(m_2) \rightarrow n\pi \qquad \text{(III.3.1)}$$

where $F_1(m_1)$ is a fireball of mass m_1, of four-momentum q_1, of isospin I_1, of G-parity G_1 and $P(m_2)$ is a light particle of mass m_2, of four-momentum q_2, of isospin I_2, of G-parity G_2 and of spin S_2.

Generalizing equation (II.3.2) to include isospin and G-parity conservation and making use of the appropriate Clebsch-Gordan coefficients, we obtain the probability for such an event:

$$\begin{aligned} P_n(M,I,G) = \frac{1}{\rho(M,I,G)} \sum_{P(m_2)} (2S_2+1) \frac{V}{(2\pi)^3} \int dm_1 dm_2 \rho(m_2) \\ \times d^3q_1 d^3q_2 \delta^3(\vec{q}_1+\vec{q}_2) \delta(M-E_1-E_2) \delta_{G,G_1G_2} \\ \times \Big[\delta_{I0} \Big[\delta_{I_20} \rho(m_1,0,G_1) P_{n-n_2}(m_1,0,G_1) \\ + \delta_{I_21} \rho(m_1,1,G_1) P_{n-n_2}(m_1,1,G_1) \Big] \\ + \delta_{I1} \Big[\delta_{I_20} \rho(m_1,1,G_1) P_{n-n_2}(m_1,1,G_1) \\ + \delta_{I_21} \Big(\rho(m_1,0,G_1) P_{n-n_2}(m_1,0,G_1) \\ + \rho(m_1,1,G_1) P_{n-n_2}(m_1,1,G_1) \Big) \Big] \Big] \end{aligned} \qquad \text{(III.3.2)}$$

where we have summed over all possible light particles. Here,

$\rho(m_2)$ is the mass distribution of the light particle. We shall use a Dirac delta function for pions and very narrow resonances and a Breit-Wigner distribution otherwise. n_2 is the number of pions coming from the decay of $P(m_2)$. The 1/2! factor does not appear because the two particles are different: $P(m_2)$ is a discrete hadron while $F_1(m_1)$ is in the continuum. We now define an auxiliary probability:

$$\tilde{P}_n(M,I,G) \equiv \rho(M,I,G)P_n(M,I,G) \qquad \text{(III.3.3)}$$

After integration over the phase-space factor, equation (III.3.2) becomes:

$$\begin{aligned}\tilde{P}_n(M,I,G) = {} & \sum_{P(m_2)} (2S_2+1) \int dm_1 dm_2 \rho(m_2) A(M,m_1,m_2) \delta_{G,G_1G_2} \\ & \times \Big[\delta_{I0}\Big[\delta_{I_2 0}\tilde{P}_{n-n_2}(m_1,0,G_1) + \delta_{I_2 1}\tilde{P}_{n-n_2}(m_1,1,G_1)\Big] \\ & + \delta_{I1}\Big[\delta_{I_2 0}\tilde{P}_{n-n_2}(m_1,1,G_1) + \delta_{I_2 1}\Big(\tilde{P}_{n-n_2}(m_1,0,G_1) \\ & + \tilde{P}_{n-n_2}(m_1,1,G_1)\Big)\Big]\Big] \qquad \text{(III.3.4)}\end{aligned}$$

where $A(M,m_1,m_2)$ is the two-body phase-space factor:

$$A(M,m_1,m_2) = \frac{V}{(2\pi)^3}\frac{\pi}{2M^4}\left[M^4-(m_1^2-m_2^2)^2\right]\lambda^{\frac{1}{2}}(M_2,m_1^2,m_2^2) \qquad \text{(III.3.5)}$$

We thus obtain an expression, in fact a recursion relation, independent of the density of states of any fireball. This is very interesting since, given appropriate initial conditions, it provides us with a way of calculating explicitly the density of states for any M, I and G. Indeed, clearly, if we sum over all values of n, we shall have summed over all possibilities of decay of a fireball with such mass and quantum numbers. Hence, we have:

$$\sum_n P_n(M,I,G) = 1 \qquad \text{(III.3.6)}$$

and from equation (III,3.3):

$$\sum_n \hat{P}_n(M,I,G) = \rho(M,I,G) \qquad \text{(III.3.7)}$$

Therefore, the probability that a fireball decays into n pions will be given by:

$$P_n(M,I,G) = \frac{\hat{P}_n(M,I,G)}{\sum_n \hat{P}_n(M,I,G)} \qquad \text{(III.3.8)}$$

III-4 Calculation of the density of states.

In the linear bootstrap, as we have seen, a fireball emits a pion or a discrete resonance leaving another fireball as a daughter. Every resonance with compatible quantum num-

bers can be produced. Here, we shall allow for the emission of π, η, ρ, ω, η', δ, f, A_2 and g. All these resonances have a width of the order of the pion mass or less. Resonances such as ε, A_1, ρ' and A_3 with larger widths have never been established as definite resonances and shall be interpreted as kinematical effects. We shall see later that, for instance, A_1 and A_3 are indeed predicted by the statistical bootstrap model as statistical enhancements.

We shall neither allow for the production of strange fireballs which, according to Zweig's rule, are strongly suppressed - thus direct emission of kaons or of strange resonances will not be taken into account - nor for the emission of non-strange resonances such as S^*, ϕ and D which decay mainly into kaons. Empirically we know that at high energy the amount of kaons is about ten times smaller than the amount of pions [3.7]. On the other hand, our model does not reflect this SU(3) symmetry breaking in the coupling constants and would overestimate the amount of kaons produced. Finally, due to their high masses, baryon production is negligible, at least in the relatively low-mass range we shall be considering.

Therefore, the only vertices considered are those in figure (3.3) where the branching ratios of the discrete resonances into pions that we have used are shown. In these, photons have been counted as neutral pions. Making use of the appropriate Clebsch-Gordan coefficients, the recursion relation

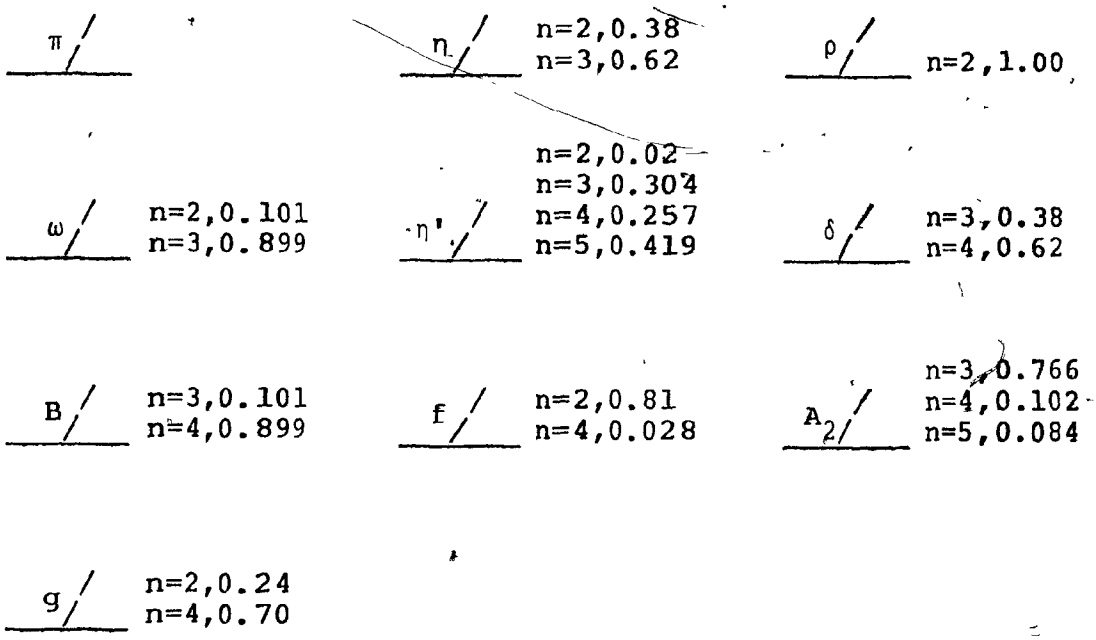

Figure 3.3: Vertices taken into account in the linear bootstrap model to calculate the total density of states. Branching ratios into different numbers of pions are also given.

(III.3.4) becomes:

$$\hat{P}_n(M,I,G) = \int_{m_{min}}^{M-m_\pi} dM' A(M,M',m_\pi)\Big[\delta_{I0}\hat{P}_{n-1}(M',1,-G)+\delta_{I1}\Big[\hat{P}_{n-1}(M',0,-G) + \hat{P}_{n-1}(M',1,-G)\Big]\Big] + \int_{m_{min}}^{M-m_\eta} dM' A(M,M',m_\eta)$$

$$\times\Big[0.38\Big[\delta_{I0}\hat{P}_{n-2}(M',0,G)+\delta_{I1}\hat{P}_{n-2}(M',1,G)\Big] + 0.62\Big[\delta_{I0}\hat{P}_{n-3}(M',0,G)+\delta_{I1}\hat{P}_{n-3}(M',1,G)\Big]\Big]$$

$$+ 3\int_{m_{min}}^{M-2m_\pi} dM' \int_{2m_\pi}^{M-M'} dm_\rho \rho(m_\rho) A(M,M',m_\rho)\Big[\delta_{I0}\hat{P}_{n-2}(M',1,G) + \delta_{I1}\Big[\hat{P}_{n-2}(M',0,G)+\hat{P}_{n-2}(M',1,G)\Big]\Big]$$

$$+ 3\int_{m_{min}}^{M-m_\omega} dM' A(M,M',m_\omega)\Big[0.101\Big[\delta_{I0}\hat{P}_{n-2}(M',0,-G) + \delta_{I1}\hat{P}_{n-2}(M',1,-G)\Big] + 0.899\Big[\delta_{I0}\hat{P}_{n-3}(M',0,-G) + \delta_{I1}\hat{P}_{n-3}(M',1,-G)\Big]\Big] + \int_{m_{min}}^{M-m_\eta'} dM' A(M,M',m_\eta')$$

$$\times\Big[0.02\Big[\delta_{I0}\hat{P}_{n-2}(M',0,G)+\delta_{I1}\hat{P}_{n-2}(M',1,G)\Big] + 0.304\Big[\delta_{I0}\hat{P}_{n-3}(M',0,G)+\delta_{I1}\hat{P}_{n-3}(M',1,G)\Big] + 0.257\Big[\delta_{I0}\hat{P}_{n-4}(M',0,G)+\delta_{I1}P_{n-4}(M',1,G)\Big]$$

$$+ 0.419\left[\delta_{I0}\hat{P}_{n-5}(M',0,G)+\delta_{I1}\hat{P}_{n-5}(M',1,G)\right]$$

$$+\int_{m_{min}}^{M-m_\delta} dM' A(M,M',m_\delta)\left[0.38\left[\delta_{I0}\hat{P}_{n-3}(M',1,-G)\right.\right.$$

$$\left.+\delta_{I1}\left[\hat{P}_{n-3}(M',0,-G)+\hat{P}_{n-3}(M',1,-G)\right]\right]$$

$$+ 0.62\left[\delta_{I0}\hat{P}_{n-4}(M',1,-G)+\delta_{I1}\left[\hat{P}_{n-4}(M',0,-G)\right.\right.$$

$$\left.\left.+\hat{P}_{n-4}(M',1,-G)\right]\right] + 3\int_{m_{min}}^{M-m_B} dM' A(M,M',m_B)$$

$$x\left[0.101\left[\delta_{I0}\hat{P}_{n-3}(M',1,G)+\delta_{I1}\left[\hat{P}_{n-3}(M',0,G)\right.\right.\right.$$

$$\left.\left.+\hat{P}_{n-3}(M',1,G)\right]\right] + 0.899\left[\delta_{I0}\hat{P}_{n-4}(M',1,G)\right.$$

$$\left.+\delta_{I1}\left[\hat{P}_{n-4}(M',0,G)+\hat{P}_{n-4}(M',1,G)\right]\right]$$

$$+ 4.05\int_{m_{min}}^{M-2m_\pi} dM' \int_{2m_\pi}^{M-M'} dm_f \rho(m_f) A(M,M',m_f)$$

$$x\left[\delta_{I0}\hat{P}_{n-2}(M',0,G)+\delta_{I1}\hat{P}_{n-2}(M',1,G)\right]$$

$$+ 0.14\int_{m_{min}}^{M-m_f} dM' A(M,M',m_f)\left[\delta_{I0}\hat{P}_{n-4}(M',0,G)\right.$$

$$\left.+\delta_{I1}\hat{P}_{n-4}(M',1,-G)\right] + 5\int_{m_{min}}^{M-m_{A_2}} dM' A(M,M',m_{A_2})$$

$$x\left[0.766\left[\delta_{I0}\hat{P}_{n-3}(M',1,-G)+\delta_{I1}\left[\hat{P}_{n-3}(M',0,-G)\right.\right.\right.$$

$$+ \hat{P}_{n-3}(M',1,-G)\Big]\Big] + 0.102\Big[\delta_{I0}\hat{P}_{n-4}(M',1,-G)$$

$$+ \delta_{I1}\Big[\hat{P}_{n-4}(M',0,-G)+\hat{P}_{n-4}(M',1,-G)\Big]$$

$$+ 0.084\Big[\delta_{I0}\hat{P}_{n-5}(M',1,-G)+\delta_{I1}\Big[\hat{P}_{n-5}(M',0,-G)$$

$$+ \hat{P}_{n-5}(M',1,-G)\Big]\Big] + 1.68\int_{m_{min}}^{M-2m_\pi} dM'$$

$$\times \int_{2m_\pi}^{M-M'} dm_g \rho(m_g) A(M,M',m_g)\Big[\delta_{I0}\hat{P}_{n-2}(M',1,G)$$

$$+ \delta_{I1}\Big[\hat{P}_{n-2}(M',0,G)+\hat{P}_{n-2}(M',1,G)\Big]\Big]$$

$$+ 4.9\int_{m_{min}}^{M-m_g} dM' A(M,M',m_g)\Big[\delta_{I0}\hat{P}_{n-4}(M',1,G)$$

$$+ \delta_{I1}\Big[\hat{P}_{n-4}(M',0,G) + \hat{P}_{n-4}(M',1,G)\Big]\Big]$$

$$+ \hat{P}_n^{init}(M,I,G) \qquad \text{(III.4.1)}$$

where $\rho(m)$ is taken to be a relativistic Breit-Wigner distribution as in equation (II.2.9) [3.8] :

$$\rho(m) = \frac{2mm_0}{\pi} \frac{\Gamma(m)}{(m_0^2-m^2)^2+m_0^2\Gamma^2(m)} \qquad \text{(III.4.2)}$$

$\Gamma(m)$ is given by:

$$\Gamma(m) = \Gamma_0 \left(\frac{q}{q_0}\right)^{2l+1} \frac{2q_0^2}{(q^2+q_0^2)} \qquad \text{(III.4.3)}$$

where

$$q = \frac{1}{2m} \lambda^{\frac{1}{2}}(m^2, m_1^2, m_2^2) \qquad \text{(III.4.4)}$$

and

$$q_0 = \frac{1}{2m} \lambda^{\frac{1}{2}}(m_0^2, m_1^2, m_2^2) \qquad \text{(III.4.5)}$$

Γ_0 and l are respectively the width at $m=m_0$ and the spin of particle m_0 while m_1 and m_2 are the masses of its decay products. This form has originally been used for the ρ resonance [3.9] but we shall adopt it for any two-body resonance of spin 1.

In equation (III.4.1), the lower limit of integration m_{min} is simply determined by the zeros of $\lambda^{\frac{1}{2}}(M^2, M'^2, m^2)$ contained in $A(M,M',m)$. Also, the mass distribution of very narrow resonances like π, η, ω, η' have been taken to be Dirac delta functions and were readily integrated over. Dirac delta functions have also been used for other resonances which start contributing to $\hat{P}_n(M,I,G)$ at n=6 or higher. Their production rates are small and the use of a finite width would

not change anything in the result while complicating its evaluation.

The initial conditions necessary to calculate $\hat{P}_n(M,I,G)$, i.e. the vertices appearing at the end of the chain (figure A.1) are collected in appendix I. Using these, equation (III.4.1) has been evaluated by computer.

However, before presenting the results, we would like to comment about the region of validity of this formula. Since in our model, fireballs contain at least a heavy resonance in addition to another particle, it is clear that equation (III.4.1) cannot describle the physical low-mass density of states. Indeed, this part of the spectrum is dominated by discrete resonances such as π, ρ, ω etc. which may contain less than three pions and are not generated by our recursion relation. These particles anyhow contribute to the total density of states and have to be taken into account if low-mass calculations are to be performed.

III-4-A The Resulting Density of States.

Figure I shows the resulting density of states (equation III.3.7). A summation up to n=15 has been necessary to ensure a very good convergence over the whole range considered. We have used a volume of radius 1.1 fm. This very reasonable value has been favored by Margolis et al. in e^+e^- annihilation [3.6] as well as in other reactions [3.10].

We observe a rather weak dependence on the quantum numbers of the fireball above 1.6 GeV. Indeed, both I=0 and I=1 curves can clearly be parametrized with the same function and the same parameters except for overall normalization constants which will differ slightly. We note also a complete independence of the G-parity for each isospin. Below 1.6 GeV, the situation is completely different and the density of states depends more strongly on the fireball quantum numbers. This is because we are in a region where new channels still appear in a discrete fashion and individual threshold effects are noticeable.

However, Hamer and Frautschi [2.9] using a different technique in which a realistic low-mass spectrum of SU(3) multiplets of mesons is fed as an input to generate higher mass states, found that the density of states reaches its asymptotic behavior at even lower-mass, i.e. at about 700 MeV. Moreover, Hagedorn [3.11] found that a smoothed experimental spectrum of resonances could be fitted down to almost the pion mass with a density of the form:

$$\rho(M) = \frac{a_0}{(M_0+M)^{5/2}} e^{M/T} \qquad \text{(III.4.6)}$$

This parametrization is off by a power of ½ from the true asymptotic form (which was not known in those days) but is very close to it over a small energy range.

In our case, we see that the analytic asymptotic solution (equation II.3.4) is entirely consistent with our calculation and we find a limiting temperature of 160 MeV, in agreement with previous estimates [2.4,2.9,3.6].

Thus, in view of the above discussion, we propose to use the asymptotic density of states (corrected for very low mass) over the entire range (dashed line on figure I). It is clear, however, that a full statistical behavior is not expected to set in in the discrete resonance region and that results obtained there should be interpreted cautiously.

III-5 Multipion Production.

We now proceed to evaluate the production cross-section of n charged pions. Only a subset of all diagrams building up the total density of states contribute to such exclusive channels. In pion-proton scattering (n is odd), the only vertices contributing are those shown in figure (3.4). We shall write a recursion relation similar to equation (III.4.1) with the following difference: since the only particles produced are either charged pions or resonances decaying into charged pions only, it is clear that we no longer have isospin symmetry (insured by the presence of the neutral pions). However, interestingly, it turns out that it is possible to write two different recursion relations, each being independent of the third component of isospin and actually of the G-parity as well

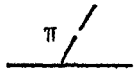

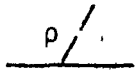

n=2,1.00

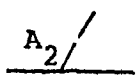

n=3,0.709

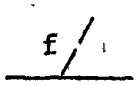

n=2,0.81
n=4,0.028

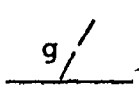

n=2,0.24
n=4,0.70

Figure 3.4: Vertices contributing to the calculated exclusive channels in the linear bootstrap model. Branching ratios into different numbers of pions are also given.

(for an additional simplification). The first holds for odd numbers of pions and the second for even numbers. These relations are:

$$\tilde{P}_n(M,1) = \int_{m_{min}}^{M-m_\pi} dM' A(M,M',m_\pi)\left[\tilde{P}_{n-1}(M',0)+0.5\,\tilde{P}_{n-1}(M',1)\right]$$

$$+ 1.5\int_{m_{min}}^{M-2m_\pi} dM' \int_{2m_\pi}^{M-M'} dm_\rho \rho(m_\rho) A(M,M',m_\rho)\tilde{P}_{n-2}(M',1)$$

$$+ 1.7725\int_{m_{min}}^{M-m_{A_2}} dM' A(M,M',m_{A_2})\left[\tilde{P}_{n-3}(M',0)\right.$$

$$\left. + 0.5\,\tilde{P}_{n-3}(M',1)\right] + 4.05\int_{m_{min}}^{M-2m_\pi} dM' \int_{2m_\pi}^{M-M'} dm_f \rho(m_f)$$

$$\times A(M,M',m_f)\tilde{P}_{n-2}(M',1) + 0.14\int_{m_{min}}^{M-m_f} dM' A(M,M',m_f)$$

$$\times \tilde{P}_{n-4}(M',1) + 0.84\int_{m_{min}}^{M-2m_\pi} dM' \int_{2m_\pi}^{M-M'} dm_g \rho(m_g)$$

$$\times A(M',M',m_g)\tilde{P}_{n-2}(M',1) + 2.45\int_{m_{min}}^{M-m_g} dM' A(M,M',m_g)$$

$$\times \tilde{P}_{n-4}(M',1) + \tilde{P}_n^{init}(M,1) \quad \text{(if n is odd)}$$

(III.5.1)

$$\tilde{P}_n(M,I) = \int_{m_{min}}^{M-m_\pi} dM' A(M,M',m_\pi)\left[\delta_{I0}(0.6667)\tilde{P}_{n-1}(M',1)\right.$$

$$\left. + \delta_{I1}\tilde{P}_{n-1}(M',1)\right] + 3\int_{m_{min}}^{M-2m_\pi} dM' \int_{2m_\pi}^{M-M'} dm_\rho \rho(m_\rho)$$

$$\times A(M,M',m_\rho)\left[\delta_{I0}(0.3333)\hat{P}_{n-2}(M',1)+\delta_{I1}\hat{P}_{n-2}(M',0)\right]$$

$$+ 1.773\int_{m_{min}}^{M-m_{A_2}} dM' A(M,M',m_{A_2})\left[\delta_{I0}(0.6667)\hat{P}_{n-3}(M',1)\right.$$

$$\left.+ \delta_{I1}\hat{P}_{n-3}(M',1)\right] + 4.05\int_{m_{min}}^{M-2m_\pi} dM' \int_{2m_\pi}^{M-M'} dm_f \rho(m_f)$$

$$\times A(M,M',m_f)\left[\delta_{I0}\hat{P}_{n-2}(M',0) + \delta_{I1}\hat{P}_{n-2}(M',1)\right]$$

$$+ 0.14\int_{m_{min}}^{M-m_f} dM' A(M,M',m_f)\left[\delta_{I0}\hat{P}_{n-4}(M',0)\right.$$

$$\left.+ \delta_{I1}\hat{P}_{n-4}(M',1)\right] + 1.68\int_{m_{min}}^{M-2m_\pi} dM' \int_{2m_\pi}^{M-M'} dm_g \rho(m_g)$$

$$\times A(M,M',m_g)\left[\delta_{I0}(0.3333)\hat{P}_{n-2}(M',1) + \delta_{I1}\hat{P}_{n-2}(M',0)\right]$$

$$+ 4.9\int_{m_{min}}^{M-m_g} dM' A(M,M',m_g)\left[\delta_{I0}(0.3333)\hat{P}_{n-4}(M',1)\right.$$

$$\left.+ \delta_{I1}\hat{P}_{n-4}(M',0)\right] + \hat{P}_n^{init}(M,I) \quad \text{(if n is even)}$$

(III.5.2)

We note that for odd values of n, $\hat{P}_n(M,0)=0$. Initial conditions used to evaluate these recursion relations can be found in appendix II.

III-5-A Production of Three Pions.

We present on figure II the three-pion mass spectrum predicted by our model. The main enhancement peaked at 1.12 GeV can be identified to the A_1 meson (ρ-π contribution only) and the shoulder starting at about 1.4 GeV to the A_3 meson (f-π contribution only). No g-π enhancement is visible at higher mass.

We would expect though a more accurate prediction if the three resonances ρ, f and g were replaced by the full di-pion amplitude as measured from the experimental phase-shifts [3.12]. Indeed, this would account for all interference phenomena of the different partial waves which are likely to show up in this low multiplicity state since few diagrams contribute. At higher multiplicity, we expect all interference effects to cancel out due to the large number of diagrams. However, individual partial waves should be well described and to illustrate the point, the ρ-π contribution has been separated out and normalized to the data obtained by Ballam et al. [3.13] for the A_1 (figure III). We see that the experimental peak is sharper than we predict but, nevertheless, the agreement is surprisingly good since at such low mass dynamical considerations should still play an important role.

The experimental status of the three-pion diffractive enhancements in both the A_1 and the A_3 regions is still confused [3.14]. Previous phase-shift analysis [3.15] showed

variation over the full width of the spectrum of the relative phases between the dominant partial wave and other partial waves associated with the background. We know that for a true resonance, a 90^{o} increase is expected. This observation led people to interpret these peaks as non-resonant threshold effects generated either by a fireball model such as the one exposed in this thesis [3.16] or in a multiperipheral way by the so-called Deck model [3.17] preferably in its Reggeized version [3.18]. This last model tends also to produce too broad a bump.

However, very recent works suggest on the contrary, that A_1 and perhaps A_3 are quite respectable resonances. First of all, a reanalysis [3.19] of the CERN-IHEP data, using analytic and unitary three-pion amplitudes concludes that, due to ambiguities in the fit, a resonant interpretation of the A_1 is not excluded. Secondly, a new partial wave analysis of coherent pion scattering off complex nuclei [3.20] supports the existence of resonant 1^{+} waves in the A_1 region as well as a resonance behavior of a 2^{-} state in the A_3 region. Thirdly, a backward $\rho^{o}\pi^{-}$ enhancement has been observed in the non-diffractive $\pi^{-}p \rightarrow (3\pi)^{-}p$ reaction at a mass of 1050 MeV [3.21]. The measured width of 195 ± 32 MeV is narrower than found in diffractive production but, nevertheless, the results of this experiment constitute a strong evidence that a resonant A_1 meson has been produced. Finally, a study of the decay of the

newly discovered heavy lepton $\tau(e^+e^- \to \tau^+\tau^- \to \nu\nu e + \nu\rho^o\pi)$ shows an indication of a bump in the A_1 region [3.22]. The $\rho\pi$ mass spectrum in spite of low statistics (21 events) is entirely consistent with the $\tau \to A_1\nu$ decay mode.

In conclusion, present experimental situation seems to support the existence of A_1 as a true resonance and likely, it will be fully confirmed in the near future. Actually, the discovery of this meson is of great importance for quark models and chiral symmetry [3.23]. On the other hand, it is also clear that in diffractive three-pion production, the whole enhancement cannot be resonant. In fact, the above discussion is suggestive of a large fraction of non-resonant behavior compatible with our statistical description.

III-5-B Production of Five Pions.

Figure IV shows the five-pion mass spectrum generated by our model. We display three different contributions to point out the importance of resonance emission. The upper curve is the result of the full calculation. It is a smooth but irregular shape peaked at 2.17 GeV and with two shoulders on the low-mass side. These two shoulders are due to the decay of the fireball into a pion plus another fireball- a pion plus a resonance at the end of the chain- (first term of equation III.5.1 and III.5.2), as indicated by the middle curve. It is clear however, that no significant meaning should be attached to the

second shoulder because it can so easily be destroyed by either statistical fluctuations or minor dynamical effects. We do not expect data to reproduce in detail the predictions of a statistical model at finite energies. On the other hand the lower shoulder is more pronounced and should manifest itself in the data. Other contributions such as resonance emission along the decay chain will peak at a somewhat higher mass and since there are so many of these configurations possible the full spectrum will be shifted at higher mass.

The lower curve shows also the prediction of the first term of equations (III.5.1) and (III.5.2) but here all initial conditions yielding more than three pions have been removed. This stresses the importance of adding all relevant contributions in generalizing the model to a higher number of pions produced. Indeed, integration over the spectra shows that the lower curve represents only 38.2% of the total number of five-pion events while the middle curve accounts for 58.3% of these events. Thus, 41.7% of the decays exhibit either the emission of at least one resonance along the chain or the emission of two resonances at its end, certainly not a negligeable fraction.

Finally, we reproduce in figure V the mass spectrum obtained using the analytic asymptotic density of states (equation II.3.4), (full line), along with the spectrum obtained when the calculated density of states (equation III.4.1) is

used (dashed line). Both curves have been normalized to the same peak value. We see that the differences between the two are very minor and clearly negligible in the spirit of our model.

Unfortunately, no data exist on diffractive five-pion production off a proton but there are some off nuclei. In the next chapter, we shall see how our predictions compare to them.

III-5-C Seven and Nine Pion Production.

The seven pion spectrum has been calculated up to 4.41 GeV only using the method outlined above. At higher masses, the accuracy, due to the great number of numerical integrations to be performed, starts to fail. Thus, we neglected all resonances' width, reducing ipso facto the number of integration by one. Looking at the curve in figure VI, we see that the matching is excellent and that virtually no error has been introduced in the process. The maximum of the peak occurs at 3.22 GeV and the whole spectrum is very smooth indicating that no particular sub-group of diagrams dominates its behavior over a limited range. This is confirmed by the two lower curves which display, as in figure IV, the contribution of pion emission along the decay chain alone. These contribute even less to the full spectrum than in the five-pion case and thus, mass differences between resonances and pion become less important. The middle curve accounts for 22.7% of the integrated number of

events while the lower one accounts for 15%.

Finally, we calculated the nine-pion spectrum presented on figure VII. We did not attempt to go beyond 4.41 GeV but we have enough information to know that it peaks at 4.3 GeV and that resonance emission along the decay chain or double resonance emission at the end of the chain is very important. Indeed, we found that pion emission alone contributes approximately 13% to the integrated number of events (middle curve) and it reduces to 8% when $\pi\rho$, $\pi f(f \to 2\pi)$, $\pi g(g \to 2\pi)$ are the only initial conditions taken into account (lower curve).

III-5-D Relative Cross-Sections.

Our statistical model cannot predict absolute cross-sections though it makes definite predictions on their relative size. They are simply given by the ratio of the respective integrated numbers of events. We have:

$$\frac{\sigma(\pi p \to (n_1\pi)p)}{\sigma(\pi p \to (n_2\pi)p)} = \frac{\int dM dN(\pi p \to (n_1\pi)p)/dM}{\int dM dN(\pi p \to (n_2\pi)p)/dM} \quad \text{(III.5.3)}$$

We collected in table I all cross-sections calculated relatively to the three-pion cross-section. In the nine-pion case we only have about half the spectrum and the results of the partial integration are multiplied by two. This provides us with a good estimate, probably accurate to within 30%. We

give our predictions for the three cases shown on the graphs. From the figures, it is obvious that resonance emission is becoming more important as the number of pions produced increases. This of course, should not come as a surprise since, as we said before, the mass differences between resonances and pion are less relevant for a heavy fireball.

Therefore, from the linear statistical boostrap, we have learned the following: a naive generalization of the model from the three-pion spectrum taking only into account pion emission along the decay chain (first term of equation (III.5.1) and (III.5.2)) and the corresponding initial conditions (all π-R vertices - middle curves - or π-R(R$\rightarrow 2\pi$) vertices only - lower curves) reveals itself completely inadequate to predict relative branching ratios but, on the other hand, is sufficiently accurate in predicting the masses (but not the detailed shapes) of all n-pion enhancements.

III-6 Non-Linear Statistical Bootstrap Model.

So far, we have considered only a simpler version of the model in which a fireball decays into two particles. We shall now take into account the next dominant contribution: the decay of the fireball into three objects. We know that asymptotically, 27% of the first generation particles come from a three-body decay. However, for low-mass enhancements such as the ones we are calculating, it should be considerably

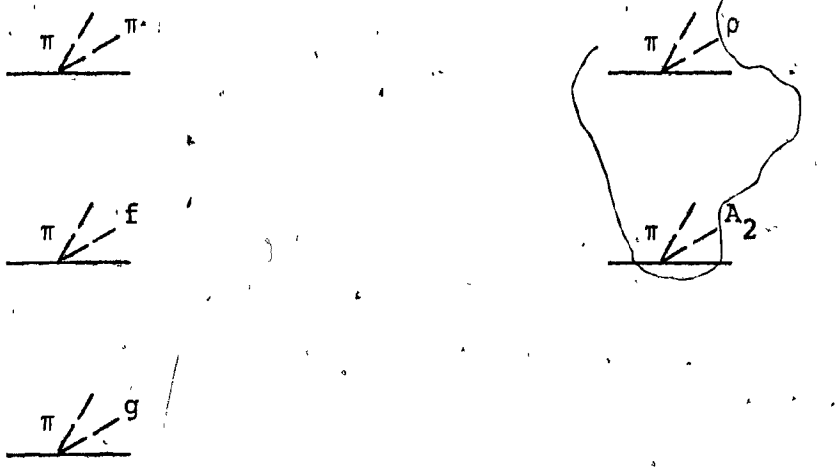

Figure 3.5: Vertices taken into account to calculate exclusive channels in the non-linear bootstrap model.

less and we shall now study how this figure is changed. In order to do so, we write recursion relations similar to equations (III.5.1) and (III.5.2), but here, we neglect all resonances' width. This is because the non-linear term is expected to contribute much less than the linear one, thus making the inclusion of widths an unnecessary complication. For the same reason, we shall not reevaluate the total density of states assuming a priori that the asymptotic temperature is not changed. From the results obtained it will be easy to judge a posteriori if this was indeed a good guess.

Along the decay chain the only vertices considered are those shown in figure 3.5. They are all of the type $\pi\pi F$ or πRF and dominate the non-linear contribution. RRF vertices are suppressed because, firstly, the integrand is smaller for larger masses and, secondly, the integration interval is narrower. However, all $\pi\pi R$, πRR and RRR vertices are allowed at the end of the chain. Initial conditions are given explicitly in appendix III. Thus, recursion relation in the non-linear version of the model are:

$$\tilde{P}_n(M,1) = 0.9\int_{m_{min}}^{M-2m_\pi} dM_1 I(M,M_1,m_\pi,m_\pi)\tilde{P}_{n-2}(M_1,1)$$

$$+ 3\int_{m_{min}}^{M-(m_\pi+m_\rho)} dM_1 I(M,M_1,m_\pi,m_\rho)\left[0.5\tilde{P}_{n-3}(M_1,0)\right.$$

$$+ 0.4\hat{P}_{n-3}(M_1,1)\Big] + 5\int_{m_{min}}^{M-(m_\pi+m_f)} dM_1 I(M,M_1,m_\pi,m_f)$$

$$\times \Big[0.81\hat{P}_{n-3}(M_1,0)+0.405\hat{P}_{n-3}(M_1,1)+0.028\hat{P}_{n-5}(M_1,0)$$

$$+ 0.014\hat{P}_{n-5}(M_1,1)\Big] + 3.191\int_{m_{min}}^{M-(m_\pi+m_{A_2})} dM_1$$

$$\times I(M,M_1,m_\pi,m_{A_2})\hat{P}_{n-4}(M_1,1) + 7\int_{m_{min}}^{M-(m_\pi+m_g)}$$

$$\times dM_1 I(M,M_1,m_\pi,m_g)\Big[0.12\hat{P}_{n-3}(M_1,0)+0.096\hat{P}_{n-3}(M_1,1)$$

$$+ 0.35\hat{P}_{n-5}(M_1,0)+0.28\hat{P}_{n-5}(M_1,1)\Big]$$

$$+ \text{terms of equation (III.5.1)} \quad \text{(if n is odd)}$$

(III.6.1)

$$\hat{P}_n(M,I) = 0.5\int_{m_{min}}^{M-2m_\pi} dM_1 I(M,M_1,m_\pi,m_\pi)\Big[\delta_{I0}\Big[0.667\hat{P}_{n-2}(M_1,0)$$

$$+ 0.333\hat{P}_{n-2}(M_1,1)\Big] + \delta_{I1}\Big[\hat{P}_{n-2}(M_1,0)+0.8\hat{P}_{n-2}(M_1,1)\Big]\Big]$$

$$+ 6\int_{m_{min}}^{M-(m_\pi+m_\rho)} dM_1 I(M,M_1,m_\pi,m_\rho)\Big[\delta_{I0}0.167\hat{P}_{n-3}(M_1,1)$$

$$+ \delta_{I1}0.4\hat{P}_{n-3}(M_1,1)\Big] + 10\int_{m_{min}}^{M-(m_\pi+m_f)} dM_1 I(M,M_1,m_\pi,m_f)$$

$$\times \Big[\delta_{I0}\Big[0.27\hat{P}_{n-3}(M_1,1)+0.009\hat{P}_{n-5}(M_1,1)\Big]$$

$$+ \delta_{I1}\left[0.405\hat{P}_{n-3}(M_1,1)+0.014\hat{P}_{n-5}(M_1,1)\right]\Big]$$

$$+ 1.7725\int_{m_{min}}^{M-(m_\pi+m_{A_2})} dM_1 I(M,M_1,m_\pi,m_{A_2})\Big[\delta_{I0}\Big[0.667$$

$$\times \hat{P}_{n-4}(M_1,0)+0.333\hat{P}_{n-4}(M,1)\Big] + \delta_{I1}\Big[\hat{P}_{n-4}(M_1,0)$$

$$+ 0.8\hat{P}_{n-4}(M_1,1)\Big]\Big] + 14\int_{m_{min}}^{M-(m_\pi+m_g)} dM_1 I(M,M_1,m_\pi,m_g)$$

$$\times\Big[\delta_{I0}\Big[0.04\hat{P}_{n-3}(M_1,1)+0.117\hat{P}_{n-5}(M_1,1)\Big]$$

$$+ \delta_{I1}\Big[0.096\hat{P}_{n-3}(M_1,1)+0.28\hat{P}_{n-5}(M_1,1)\Big]\Big]$$

$$+ \text{terms of equation (III.5.2)} \quad \text{(if n is even)}$$

(III.6.2)

where $I(M,M_1,m_a,m_b)$ is the three-body phase-space calculated in appendix IV. Factors for identical particles are included in the coefficients.

III-6-A Effect of the Non-Linear Contribution on Multipion Production.

The major conclusion that we draw from the results of this enlarged version of the model is that the non-linear term is hardly necessary unless a few percent accuracy is desired. This is, from a practical point of view, a very

interesting and fortunate conclusion indeed, since this more general model is much difficult to handle numerically requiring huge memory and long execution time. Let us now see in details its influences on our previous results.

Firstly, its effect on the shape of all spectra to which it contributes (5π and up) is totally negligible. Indeed, the new spectra, once properly renormalized, can be superimposed within plotting accuracy to the old ones establishing the smallness and the smoothness of the non-linear term.

Secondly, its effect on the magnitude of the cross-sections is also pretty small and, as expected, slowly increases with the number of pions produced or, equivalently, with the mass of the enhancement. More precisely three-particle vertices, apart from not contributing to the three-pion production cross-section, accounts for 1.5% of the five-pion spectrum; only 3% of all seven-pion events exhibit at one place or another one or more three-particle decay and it goes up to approximately 4.1% in the nine-pion case. We give in Table I the new relative cross-sections obtained in this non-linear version and a glance at it convinces us that unless very precise experimental data become available the statistical bootstrap model, in its simpler linear version, is completely satisfactory.

By the same occasion, our results provide us with a full a posteriori justification for our use of an unmodified

density of states. Indeed three-particle vertices would contribute very little to it, thus having a negligible effect on the temperature.

CHAPTER IV

APPLICATION TO PION-DEUTERON SCATTERING

IV-1 Introduction.

It is an easy matter to extend the results obtained in the previous chapter for diffractive pion-proton scattering to pion-nucleus scattering. Among the different nuclei, deuteron is particularly suitable to study diffractive dissociation and presents definite advantages on proton target. There are a number of reasons for it [4.1]. The deuteron is an isospin zero nucleus thus eliminating all non-coherent background coming from I=1 exchanges (important in pion-proton). The deuteron is a spin one nucleus for which spin-flip contributions are forbidden in the forward direction (t=0) and therefore heavily suppressed in the diffractive region (t very small). The deuteron has no excited states so that, except for few deuteron break-up events followed by recombination, vacuum quantum numbers exchange can be assumed every time a deuteron nucleus is identified in the final state. Finally, the deuteron form factor favors scattering in the small t region, thus favoring diffractive events. All these reasons combine to make easier the production (relative to other channels) and the identification of diffractive events. At least, they were sufficient to stimulate experimentalists [4.2, 4.3].

IV-2 Coherent Production on Nuclei.

Nuclei are a collection of interacting nucleons very close to each other. For this reason, we expect diffractive hadron-nucleus interactions to be more complicated than hadron-hadron collisions. However, at high energies (in the GeV range), an event takes place before any nuclear rearrangement can occur and the nucleus is seen as a frozen object. It was thus possible to develop with much success a sophisticated theory [4.4] accounting for mutual screening of nucleons and multiple scattering. It involves in general the solution of a set of coupled differential equations related to all diffractive channels that can be produced. But, as we have just seen, diffractive events are highly concentrated in the low t region, a region where production amplitudes are very dominantly coherent. Nuclear coherence implies that the outgoing particle shares with the incoming hadron all its internal quantum numbers except spin and parity since there might be some angular momentum transfer. This condition is clearly satisfied in diffraction dissociation. It also puts restrictions on the mass of the particles that can be diffractively produced. Indeed, in order to keep in phase both the incoming and the outcoming wavefunctions, the following condition must be fulfilled:

$$\Delta K \, R < 1 \qquad \text{(IV.2.1)}$$

which states that the momentum transfer cannot exceed the in-

verse of the nuclear radius. In addition, there is a minimum momentum transfer involved in any reaction where the masses of the initial and the final particles differ:

$$t_{min} = - \left[(M^2-m^2)/2p_{Lab}\right]^2 \qquad \text{(IV.2.2)}$$

Thus our coherence condition implies:

$$M^2-m^2 \lesssim 2p_{Lab}/R \qquad \text{(IV.2.3)}$$

suppressing the production of high mass states. Theory [4.4] predicts very little multiple scattering in this low t region where differential cross-sections, characterized by a steep falloff mainly determined by the nuclear form factor, can be parametrized by an exponential in t. Thus it is not necessary to use the full machinery of the theory and the following factorized form is quite sufficient [4.5]:

$$\frac{d^2\sigma_{\pi N}}{dtdM} = \left(\frac{\sigma^T_{\pi N}}{\sigma^T_{\pi p}}\right)^2 F^2(t) \frac{d^2\sigma_{\pi p}}{dtdM} \qquad \text{(IV.2.4)}$$

where F(t) is the nuclear form factor. Once integrated over t from $(-\infty)$ to t_{min}, the simple distribution results:

$$\frac{d\sigma_{\pi N}}{dM} = \left(\frac{\sigma^T_{\pi N}}{\sigma^T_{\pi p}}\right)^2 e^{-bt_{min}} \frac{d\sigma_{\pi p}}{dM} \qquad \text{(IV.2.5)}$$

where b is a parameter which can be extracted from experimental differential cross-sections. This is completely equivalent to the result obtained from the theory in the small t approximation [4.6] leading to the identification:

$$b = \frac{1}{6}\langle r^2 \rangle \qquad \text{(IV.2.6)}$$

where $\langle r^2 \rangle$ is the rms nuclear radius.

It is clear from equation (IV.2.5) that the presence of the nucleus produces a shifting on the low-mass side and a shrinking of all multipion spectra. These effects are more pronounced for higher multiplicities thus affecting the size of the relative cross-sections.

IV-3 Multipion Production in Pion-Deuteron Scattering.

We shall now present our predictions on deuterium and compare them with data when available. We emphasize that no additional free parameters are introduced when dealing with nuclei since both $(\sigma^T_{\pi D}/\sigma^T_{\pi p})^2$ and b (or $\langle r^2 \rangle$) are taken from experiments. The ratio of the deuteron to proton square cross-sections is equal to $\sim$3.6 [4.7] and the value of b has been determined [4.2,4.3,4.8] to be 30-32 corresponding to a radius of approximately 2.7 fm. Margolis and Rudaz [4.6] used a radius of 2.8 fm (b=33.7) which is equally good since, as we shall see, our results are little sensitive to a precise value.

In the predicted spectra presented in figures VIII-XI, b=31 was selected. In figure VIII, we compare our three-pion mass spectrum with data (p_{Lab}=15 GeV/c) [4.3] of the LPS#1 sector since our model does not attempt to describe the entire three-pion channel (for instance no d* formation is taken into account). We do not obtain a very good agreement. The width is too big mainly because the f-π enhancement measured at 1.65 GeV manifests itself as a smooth shoulder from 1.4 GeV on. However Harris et al. [4.1,4.3], using the full dipion amplitude as discussed in chapter II, reproduced very well the experimental result suggesting that interference effects are indeed important at low multiplicity. While most people seem to prefer a Deck mechanism to describe this channel, it is found that the statistical bootstrap model makes a satisfactory job in the forward LPS sector. Of course, in other sectors, the Deck model is superior since it incorporates d* effects.

However at higher multiplicity our predictions should improve considerably due to the large number of diagrams contributing. Figure IX which displays the five-pion spectrum indicates that this is indeed the case. The agreement with data [4.3] is excellent, even structure details usually associated with dynamical effects are very satisfactorily explained: the peak of the enhancement is observed at precisely the predicted mass (2.12 GeV); a prominent shoulder on the low-mass side is seen to have at least mostly a statistical origin: the

competition of classes of diagrams peaking at somewhat different masses (see chapter II, we note that this shoulder is further enhanced in pion-deuteron than in pion-proton scattering by the nuclear form factor); the slope on the high mass side follows closely the data up to 3.0 GeV. It is not perfect though and if the few unexplained events in the shoulder region could mostly disappear in a higher statistics experiment [4.9], it is doubtful that those in the tail will. For instance, the latter could be connected to some d* effects produced in minimal quantity and not accounted for in our model. or to some coherence setting up among the different partial waves. According to duality, this leads to a power-law behavior, typical of a Regge tail [2.1]. Obviously, little attention should be paid to the predicted double peak. It is simply the reflection of the small shoulder in the pion-proton spectrum enhanced by the deuteron form factor and would disappear with it for the same reasons.

Therefore, we conclude that the main features of this enhancement are statistical in nature and thus little dynamics is involved in the process. Once again, our results stress the importance of many relatively small contributions adding up together and responsible of structure details formation. The obtained agreement with data can be regarded as remarkable for, as far as we know, no other model gives such a good description of the five-pion enhancement. In particular, different multi-

peripheral mechanisms have been tried [4.1b,4.3b] with rather modest success. Two of them were two-body versions ($g\pi,\rho\pi$), but no such dominant quasi two-body states were identified in the data while the third one ($\rho\rho\pi$) predicts too many ρ's. In addition, none of these fits well the five-pion distribution.

The next two figures show the seven and nine pion spectra respectively. Clearly, no specific comments are needed. Both are very smooth and, as expected from the deuteron form factor, at masses several hundreds MeV lower than their pion-proton counterparts: the seven pion bump peaks at 2.72 GeV and the nine pion one at 3.22 GeV.

IV-4 Relative Cross-Sections.

Relative pion production cross-sections off deuteron are easily obtained from integration of equation (IV.2.5). Several conclusions can be drawn from the results presented in table II. Two of them are already known from our previous analysis of pion-proton scattering, i.e. the importance of resonance emission which increases by almost a factor of three the number of five-pion events and by roughly an order of magnitude the nine-pion cross-section; the negligibility of three-particle vertices whose contribution amounts only to a few percent. A third one is the little sensitivity of all cross-sections to the actual slope of the deuteron form factor. This can be seen from a comparison of the values obtained

using b=31 with those calculated with b=33.67 ($\langle r^2 \rangle^{\frac{1}{2}}$=2.8fm): a mere 5% variation in the ratio $\sigma(3\pi)/\sigma(5\pi)$ and approximately 30% in $\sigma(3\pi)/\sigma(9\pi)$. Thus in view of the extreme difficulty to obtain an accurate nine-pion cross-section measurement, it is obvious that 30% represents a really small change and that one does not have to worry too much about the precise slope value. Our fourth conclusion is that measurements of multiplicities higher than five will be quasi impossible [4.10] in this energy range (p_{Lab}=15GeV/c) since, relative to the number of five-pion events, only 1.6% yield seven pions. However, we have calculated that 21% of the absolute number of five-pion events obtained at p_{Lab}=15GeV/c is reached in the seven-pion channel if p_{Lab}=50GeV/c is used. At 100 GeV/c, this ratio goes up to 28% and thus we believe such an experiment could be performed with success at, for instance, Fermilab. In addition we note that the deuteron still remains a better target than a proton since the latter yields only 9% in its asymptotic regime.

The only available piece of data is the relative three to five-pion cross-section. Lubatti and his collaborators [4.3] measured a ratio of 17.4±3.5 in excellent agreement with our predictions independently of the selected model's version. These same authors, following Margolis and Rudaz [4.6], estimated this ratio to be 42 assuming that the simplest version of the model (4th column in tables I and II) was largely dominant. In order to explain the discrepancy, they suggested an increase of the fireball radius neglecting its relation with temperatu-

re [2.9]. As we have seen, this is not at all necessary since a correct application of the model leads to the right value.

In summary, we showed that the statistical bootstrap model gives a good description of experimental data available so far, in particular of the five-pion enhancement, giving great confidence in our higher multiplicity predictions. The detailed shape of the three-pion spectrum in the LPS#1 sector is better accounted for if the full dipion amplitude is used rather than the discrete resonances produced in the reaction. The three to five-pion ratio is very well predicted by our model suggesting some sort of precocious statistical behavior due to the rapid reach of the asymptotic density of states, certainly the best applicability criterion for our statistical model. While the three-pion enhancement is basically two-body states easily separable, we found the five-pion one to be the sum of many diagrams of different numbers of steps in the decay cascade with no single contribution really dominating. This is in agreement with experiment [4.3] and in contrast with many versions of the Deck mechanism. In this regard, seven-pion measurements will be very interesting since, if this behavior persists, the statistical bootstrap model will provide a very reliable tool to predict the characteristics of high multiplicity diffractive dissociation.

CHAPTER V

SUMMARY AND CONCLUSIONS

In this thesis, we studied diffractive multipion production resulting in low-mass enhancements. In order to do so, a hybrid model was developed in which a dense set of overlapping resonances is formed by Regge exchange in the t-channel and then decays statistically into multipion states in the s-channel. Isospin and G-parity conservation were fully taken into account as well as the finite width of discrete resonances produced in the reaction. A factorized form of the cross-section (equation II.2.16) was obtained, consequence of the independence of fireball formation and decay. Indeed, we assumed that the fireball is sufficiently long-lived to "forget" the way it was formed. Due to the great number of open channels, the probability of decaying into a specific channel is simply proportional to the number of configurations assumed by this channel and inversely proportional to the total number of configurations. Since the total density of states grows exponentially within powers of M, thus suppressing high mass states, low-mass threshold enhancements result. The general formalism of the model as well as a brief discussion of the statistical bootstrap of Hagedorn and Frautschi which we used to calculate densities of states was presented in chapter II.

We next considered application to diffractive pion-pro-

ton scattering for which a triple-Pomeron exchange was selected, as suggested by previous analyses, for fireball formation and proceeded to calculate explicitly the total density of states in the linear version of the model. For this purpose, we wrote a recursion relation (equation III.4.1) allowing us to generate any multiplicity state of any isospin and G-parity. We found that all curves could be fitted by the same function using the same values of the parameters except for a small change in the normalization constants of the I=0 and I=1 densities. The asymptotic temperature turned out to be 160 MeV (for a radius of 1.1 fm) in agreement with previous calculations. Our approach was not suited for the low-mass region since it does not account for discrete resonances but a direct counting of states by Hagedorn led us to conclude that the analytic asymptotic density of states ($ae^{M/T}/M^3$) corrected for very low masses could be used over the entire mass range.

The occupied number of states was then calculated and even though isospin symmetry was no longer present, we were able to write two different recursion relations, each of which turning out to be G-parity independent thus simplifying their evaluation.

Using these, the three, five, seven and nine-pion mass spectra were obtained as well as the relative cross-sections. Our results led us to the following conclusions:

1- Diffractive production of A_1, if its existence as a true resonance is confirmed, is accompanied by the

production of a large non-resonant background satisfactorily described by the statistical bootstrap model.

2- The experimental three-pion enhancement is better described if the full dipion amplitude is used rather than the discrete resonances ρ, f and g [5,1]. This is suggestive of important interference effects among these resonances observable at low multiplicity due to the small number of contributing diagrams.

3- Resonance emission along the decay chain and double resonance production at the end of the chain are very important at high multiplicity ($n \geq 5$). Due to the great number of possible diagrams, they actually account for most of the cross-section (though a little more than 40% in the n=5 case). However, the simplest version of the model (pion emission along the decay chain; $\pi\rho$, $\pi f (f \to 2\pi)$, $\pi g (g \to 2\pi)$ at the end) is sufficient to determine with a good accuracy the mass of all enhancements.

4- Structure details in the five-pion enhancement are due to competition between different classes of diagrams peaking at somewhat different masses. At higher multiplicity, no such details are observed since mass differences between pion and resonances

become less relevant.

5- The contribution of the non-linear terms (three-particle vertices) is negligible unless a few per-cent accuracy is needed. They do not alter the shape of any n-pion mass distributions and can be superimposed within plotting accuracy to the predictions of the linear version provided a suitable renormalization of the peak values is performed.

In chapter IV, our analysis of pion-proton collision was extended to coherent pion-deuteron scattering. Because very small values of t are favored in diffractive processes, double scattering is negligible and it was quite sufficient to simply multiply our results on hydrogen by an exponential in t to approximate the deuteron form factor (equation IV.2.5). By doing so, no arbitrariness was introduced in the model since the two needed extra parameters were taken from experiment. Conclusions and comments suggested by our results go as follows:

1- The nuclear form factor produces a shifting on the low-mass side and a shrinking of mass spectra more pronounced at high multiplicity thus changing the size of the relative cross-sections. However, as expected, all conclusions drawn from pion scattering off a proton remain valid on a deuteron target.

2- The statistical model gives a satisfactory description of the three-pion spectrum in the forward LPS

sector. It cannot account for the entire channel since no d* production is incorporated.

3- The predicted five-pion mass distribution agrees very well with data. No two-body states dominate the channel as confirmed by experiment. Most structure details are found to have a statistical origin indicating that little dynamics is involved in high multiplicity diffractive enhancements and giving great confidence in our seven and nine-pion predictions. The last point is further supported by our next conclusion.

4- The three to five-pion cross-section ratio, $\sigma(3\pi)/\sigma(5\pi)=16.94$ (non-linear version, b=31) is in excellent agreement with the measured value 17.4 ± 3.5. This is suggestive of precocious statistical behavior due to the rapid reach of the asymptotic density of states.

5- A precise determination of the slope value of the deuteron form factor is of minor importance in the statistical bootstrap model unless very high multiplicity experiments are made.

6- Measurements of multiplicities higher than five will have to be performed at $P_{Lab}>50$ GeV/c to get a sufficient number of events. Moreover, the deuteron still remains a better target than the proton.

These measurements will be extremely useful for our understanding of diffractive dissociation. We presented a model in which higher multiplicity enhancements are generated from lower ones in a completely determined fashion. Because of its statistical nature, the accuracy of its predictions should improve with multiplicity making comparison with experiment more stringent. In particular, the existence of fireballs, crucial in our type of model, remains to be experimentally established. For the time being, we have every reason to believe that it is indeed a good concept.

Though very well suited for pion diffractive dissociation, the statistical bootstrap model is not limited to it and can be used to explore other kinds of reactions such as, for instance, photon dissociation. Some work has already been done in this connection [5.2], on a beryllium target (NAL data, reference 5.3) and we would like to end by stating our preliminary results [5.4]:

The four-pion enhancement, known as the $\rho'(1600)$, cannot adequately be described by our model, we predict too wide a distribution, most likely it is a true resonance. However, a large background of statistical nature, which we estimated roughly to be of the same order of magnitude as the measured cross-section, might be simultaneously produced. This could explain why it is experimentally so difficult to establish the $\rho'(1600)$ resonance status.

APPENDIX I

Initial Conditions in the Linear Bootstrap (Density of states).

We state here the non-zero initial conditions used to evaluate the density of states in the linear bootstrap model (eq.III.4.1). They correspond to the diagrams of figure (A.1). The following notation is adopted:

$$PI(M,m_1,m_2) = \int_{m_3+m_4}^{M-(m_5+m_6)} dm_1' \rho(m_1') \int_{m_5+m_6}^{M-m_1'} dm_2' \rho(m_2') A(M,m_1',m_2') \tag{A.1}$$

where m_3 and m_4 are the masses of the decay products of particle 1 and m_5 and m_6 those of particle 2. $\rho(m)$ is taken to be a Dirac delta function for the very narrow resonances π,η,ω,η'; a Breit-Wigner distribution for ρ,δ,B and A_2 in vertices contributing to $\hat{P}_4(M,I,G)$ or lower and a Dirac delta function for all particles in vertices contributing to $\hat{P}_5(M,I,G)$ or higher. Making use of the appropriate spins and Clebsch-Gordon coefficients and dividing by 2! when two particles are identical, we obtain:

$$\hat{P}_3(M,0,-) = 3PI(M,m_\rho,m_\pi) + 1.68\ PI(M,m_g(g \to 2\pi),m_\pi)$$

$$\hat{P}_3(M,1,+) = 0.303\ PI(M,m_\omega,m_\pi)$$

$$\tilde{P}_3(M,1,-) = 0.38\ PI(M,m_\eta,m_\pi) + 3\ PI(M,m_\rho,m_\pi) + 0.02\ PI(M,m_{\eta'},m_\pi)$$
$$+ 4.05\ PI(M,m_f(f\to 2\pi),m_\pi) + 1.68\ PI(M,m_g(g\to 2\pi),m_\pi)$$

$$\tilde{P}_4(M,O,+) = 0.38\ PI(M,m_\delta,m_\pi) + 3.545\ PI(M,m_{A_2}(A_2\to\rho+\pi),m_\pi)$$
$$+ 0.285\ PI(M,m_{A_2}(A_2\to\eta+\pi),m_\pi) + 0.072\ PI(M,m_\eta,m_\eta)$$
$$+ 0.008\ PI(M,m_\eta,m_{\eta'}) + 1.539\ PI(M,m_f(f\to 2\pi),m_\eta)$$
$$+ 4.5\ PI(M,m_\rho,m_\rho) + 5.04\ PI(M,m_g(g\to 2\pi),m_\rho)$$
$$+ 0.046\ PI(M,m_\omega,m_\omega) + 0.081\ PI(M,m_f(f\to 2\pi),m_{\eta'})$$
$$+ 8.201\ PI(M,m_f(f\to 2\pi),m_f(f\to 2\pi))$$
$$+ 1.411\ PI(M,m_g(g\to 2\pi),m_g(g\to 2\pi))$$

$$\tilde{P}_4(M,O,-) = 0.303\ PI(M,m_B(\omega\to 2\pi),m_\pi) + 0.115\ PI(M,m_\omega,m_\eta)$$
$$+ 0.003\ PI(M,m_\omega,m_{\eta'}) + 1.227\ PI(M,m_f(f\to 2\pi),m_\omega)$$

$$\tilde{P}_4(M,1,+) = 2.697\ PI(M,m_\omega,m_\pi) + 0.38\ PI(M,m_\delta,m_\pi)$$
$$+ 3.545\ PI(M,m_{A_2}(A_2\to\rho+\pi),m_\pi)$$
$$+ 0.285\ PI(M,m_{A_2}(A_2\to\eta+\pi),m_\pi) + 1.14\ PI(M,m_\rho,m_\eta)$$

$$+ 0.638\ PI(M,m_g(g\to 2\pi),m_\eta) + 4.5\ PI(M,m_\rho,m_\rho)$$

$$+ 0.06\ PI(M,m_\rho,m_{\eta'}) + 12.15\ PI(M,m_f(f\to 2\pi),m_\rho)$$

$$+ 5.04\ PI(M,m_g(g\to 2\pi),m_\rho) + 0.034\ PI(M,m_g(g\to 2\pi),m_{\eta'})$$

$$+ 6.804\ PI(M,m_f(f\to 2\pi),m_g(g\to 2\pi))$$

$$+ 1.411\ PI(M,m_g(g\to 2\pi),m_g(g\to 2\pi))$$

$$\tilde{P}_4(M,1,-) = 0.62\ PI(M,m_\eta,m_\pi) + 0.304\ PI(M,m_{\eta'},m_\pi)$$

$$+ 0.303\ PI(M,m_B(\omega\to 2\pi),m_\pi) + 0.909\ PI(M,m_\rho,m_\omega)$$

$$+ 0.509\ PI(M,m_g(g\to 2\pi),m_\omega)$$

$$\tilde{P}_5(M,0,+) = 0.62\ PI(M,m_\delta,m_\pi) + 0.51\ PI(M,m_{A_2},m_\pi)$$

$$+ 0.236\ PI(M,m_\eta,m_\eta) + 0.128\ PI(M,m_\eta,m_{\eta'})$$

$$+ 0.909\ PI(M,m_\rho,m_B) + 0.817\ PI(M,m_\omega,m_\omega)$$

$$+ 0.006\ PI(M,m_\eta,m_{\eta'}) + 2.511\ PI(M,m_f,m_\eta)$$

$$+ 1.231\ PI(M,m_{\eta'},m_f) + 0.509\ PI(M,m_B,m_g)$$

$$\tilde{P}_5(M,0,-) = 2.697\ PI(M,m_B,m_\pi) + 4.9\ PI(M,m_g,m_\pi)$$

$$+ 1.213\ PI(M,m_\omega,m_\eta) + 1.14\ PI(M,m_\rho,m_\delta)$$

$$+ 11.49\ PI(M,m_\rho,m_{A_2}) + 0.146\ PI(M,m_\omega,m_{\eta'})$$

$$+ 10.923\ PI(M,m_f,m_\omega) + 0.638\ PI(M,m_\delta,m_g)$$

$$+ 6.434\ PI(M,m_{A_2},m_g)$$

$$\rho_5(M,1,+) = 0.62\ PI(M,m_\delta,m_\pi) + 0.51\ PI(M,m_{A_2},m_\pi)$$

$$+ 0.115\ PI(M,m_\eta,m_B) + 1.86\ PI(M,m_\rho,m_\eta)$$

$$+ 0.312\ PI(M,m_\rho,m_{\eta'}) + 0.909\ PI(M,m_\rho,m_B)$$

$$+ 0.115\ PI(M,m_\omega,m_\delta) + 1.16\ PI(M,m_\omega,m_{A_2})$$

$$+ 0.006\ PI(M,m_{\eta'},m_B) + 1.227\ PI(M,m_B,m_f)$$

$$+ 1.042\ PI(M,m_g,m_\eta) + 0.511\ PI(M,m_g,m_{\eta'})$$

$$+ 0.509\ PI(M,m_B,m_g)$$

$$\rho_5(M,1,-) = 0.257\ PI(M,m_{\eta'},m_\pi) + 2.697\ PI(M,m_B,m_\pi)$$

$$+ 0.14\ PI(M,m_f,m_\pi) + 4.9\ PI(M,m_g,m_\pi)$$

$$+ 0.144\ PI(M,m_\delta,m_\eta) + 1.455\ PI(M,m_\eta,m_{A_2})$$

$$+ 8.091\ PI(M,m_\rho,m_\omega) + 1.14\ PI(M,m_\rho,m_\delta)$$

$$+ 11.49\ PI(M,m_\rho,m_{A_2}) + 0.092\ PI(M,m_\omega,m_B)$$

$$+ 0.008\ PI(M,m_{\eta'},m_{\delta}) + 0.077\ PI(M,m_{\eta'},m_{A_2})$$

$$+ 1.539\ PI(M,m_{\delta},m_{f}) + 15.512\ PI(M,m_{f},m_{A_2})$$

$$+ 4.531\ PI(M,m_{g},m_{\omega}) + 0.638\ PI(M,m_{\delta},m_{g})$$

$$+ 6.434\ PI(M,m_{A_2},m_{g})$$

$$\hat{P}_6(M,O,+) = 0.42\ PI(M,m_{A_2},m_{\pi}) + 0.286\ PI(M,m_{\eta},m_{\eta'})$$

$$+ 0.053\ PI(M,m_{f},m_{\eta}) + 8.091\ PI(M,m_{\rho},m_{B})$$

$$+ 14.7\ PI(M,m_{g},m_{\rho}) + 0.051\ PI(M,m_{\eta'},m_{\eta'})$$

$$+ 1.044\ PI(M,m_{\eta'},m_{f}) + 4.531\ PI(M,m_{B},m_{g})$$

$$+ 8.232\ PI(M,m_{g},m_{g}) + 0.192\ PI(M,m_{\eta},m_{\eta})$$

$$+ 3.637\ PI(M,m_{\omega},m_{\omega}) + 0.072\ PI(M,m_{\delta},m_{\delta})$$

$$+ 1.455\ PI(M,m_{\delta},m_{A_2}) + 0.046\ PI(M,m_{B},m_{B})$$

$$+ 7.334\ PI(M,m_{A_2},m_{A_2}) + 0.567\ PI(M,m_{f},m_{f})$$

$$\hat{P}_6(M,O,-) = 1.86\ PI(M,m_{\rho},m_{\delta}) + 1.53\ PI(M,m_{\rho},m_{A_2})$$

$$+ 0.898\ PI(M,m_{\omega},m_{\eta'}) + 0.042\ PI(M,m_{f},m_{\omega})$$

$$+ 1.042\ PI(M,m_{\delta},m_{g}) + 0.857\ PI(M,m_{A_2},m_{g})$$

$$+ 1.672\ PI(M,m_\omega,m_\eta) + 0.115\ PI(M,m_\delta,m_B)$$

$$+ 1.16\ PI(M,m_B,m_{A_2})$$

$$\hat{P}_6(M,1,+) = 0.42\ PI(M,m_{A_2},m_\pi) + 1.213\ PI(M,m_\eta,m_B)$$

$$+ 1.862\ PI(M,m_g,m_\eta) + 0.771\ PI(M,m_\rho,m_{\eta'})$$

$$+ 8.091\ PI(M,m_\rho,m_B) + 0.42\ PI(M,m_f,m_\rho)$$

$$+ 14.7\ PI(M,m_g,m_\rho) + 1.213\ PI(M,m_\omega,m_\delta)$$

$$+ 10.484\ PI(M,m_\omega,m_{A_2}) + 0.146\ PI(M,m_{\eta'},m_B)$$

$$+ 0.53\ PI(M,m_{\eta'},m_g) + 10.923\ PI(M,m_B,m_f)$$

$$+ 20.08\ PI(M,m_f,m_g) + 4.531\ PI(M,m_B,m_g)$$

$$+ 8.232\ PI(M,m_g,m_g) + 0.072\ PI(M,m_\delta,m_\delta)$$

$$+ 1.455\ PI(M,m_\delta,m_{A_2}) + 0.046\ PI(M,m_B,m_B)$$

$$+ 7.334\ PI(M,m_{A_2},m_{A_2})$$

$$\hat{P}_6(M,1,-) = 0.419\ PI(M,m_{\eta'},m_\pi) + 0.471\ PI(M,m_\eta,m_\delta)$$

$$+ 2.568\ PI(M,m_\eta,m_{A_2}) + 1.86\ PI(M,m_\rho,m_\delta)$$

$$+ 1.53\ PI(M,m_\rho,m_{A_2}) + 1.634\ PI(M,m_\omega,m_B)$$

$$+ 1.485\ PI(M,m_g,m_\omega) + 0.128\ PI(M,m_{\eta'},m_\delta)$$

$$+ 1.175\ PI(M,m_{\eta'},m_{A_2}) + 2.511\ PI(M,m_\delta,m_f)$$

$$+ 2.066\ PI(M,m_f,m_{A_2}) + 1.042\ PI(M,m_\delta,m_g)$$

$$+ 0.857\ PI(M,m_{A_2},m_g) + 0.115\ PI(M,m_\delta,m_B)$$

$$+ 1.16\ PI(M,m_B,m_{A_2})$$

$$\mathcal{P}_7(M,O,+) = 0.319\ PI(M,m_\eta,m_{\eta'}) + 0.087\ PI(M,m_{\eta'},m_{\eta'})$$

$$+ 1.74\ PI(M,m_{\eta'},m_f) + 0.087\ PI(M,m_f,m_\eta)$$

$$+ 0.236\ PI(M,m_\delta,m_\delta) + 2.375\ PI(M,m_\delta,m_{A_2})$$

$$+ 0.817\ PI(M,m_B,m_B) + 1.485\ PI(M,m_B,m_g)$$

$$+ 1.934\ PI(M,m_{A_2},m_{A_2})$$

$$\mathcal{P}_7(M,O,-) = 1.26\ PI(M,m_\rho,m_{A_2}) + 19.473\ PI(M,m_{A_2},m_g)$$

$$+ 0.82\ PI(M,m_\omega,m_{\eta'}) + 0.378\ PI(M,m_f,m_\omega)$$

$$+ 1.213\ PI(M,m_\delta,m_B) + 1.862\ PI(M,m_\delta,m_g)$$

$$+ 10.484\ PI(M,m_B,m_{A_2})$$

$$\mathcal{P}_7(M,1,+) = 1.257\ PI(M,m_\rho,m_{\eta'}) + 1.503\ PI(M,m_\omega,m_{A_2})$$

$$+ 2.194\ PI(M,m_\eta,,m_g) + 1.672\ PI(M,m_\eta,m_B)$$

$$+ 3.038\ PI(M,m_g,m_\eta) + 1.672\ PI(M,m_\omega,m_\delta)$$

$$+ 0.898\ PI(M,m_\eta,,m_B) + 0.236\ PI(M,m_\delta,m_\delta)$$

$$+ 3.553\ PI(M,m_\delta,m_{A_2}) + 0.817\ PI(M,m_B,m_B)$$

$$+ 0.042\ PI(M,m_B,m_f) + 1.485\ PI(M,m_B,m_g)$$

$$+ 1.953\ PI(M,m_{A_2},m_{A_2})$$

$$\tilde{P}_7(M,1,-) = 0.476\ PI(M,m_\eta,m_{A_2}) + 1.26\ PI(M,m_\rho,m_{A_2})$$

$$+ 1.148\ PI(M,m_\eta,,m_{A_2}) + 2.237\ PI(M,m_f,m_{A_2})$$

$$+ 19.473\ PI(M,m_{A_2},m_g) + 0.384\ PI(M,m_\eta,m_\delta)$$

$$+ 7.274\ PI(M,m_\omega,m_B) + 13.215\ PI(M,m_g,m_\omega)$$

$$+ 0.286\ PI(M,m_\eta,,m_\delta) + 1.213\ PI(M,m_\delta,m_B)$$

$$+ 0.053\ PI(M,m_\delta,m_f) + 1.862\ PI(M,m_\delta,m_g)$$

$$+ 10.484\ PI(M,m_B,m_{A_2})$$

$$\tilde{P}_8(M,0,+) = 0.26\ PI(M,m_\eta,m_\eta,) + 0.16\ PI(M,m_\eta,,m_\eta,)$$

$$+ 0.476\ PI(M,m_\delta,m_{A_2}) + 1.739\ PI(M,m_{A_2},m_{A_2})$$

$$+ 0.036\ PI(M, m_{\eta'}, m_f) + 0.192\ PI(M, m_\delta, m_\delta)$$

$$+ 3.637\ PI(M, m_B, m_B) + 13.215\ PI(M, m_B, m_g)$$

$$+ 0.01\ PI(M, m_f, m_f) + 12.005\ PI(M, m_g, m_g)$$

$$\hat{P}_8(M,0,-) = 1.13\ PI(M, m_\omega, m_{\eta'}) + 1.503\ PI(M, m_B, m_{A_2})$$

$$+ 1.672\ PI(M, m_\delta, m_B) + 3.038\ PI(M, m_\delta, m_g)$$

$$+ 0.071\ PI(M, m_f, m_{A_2}) + 2.499\ PI(M, m_{A_2}, m_g)$$

$$\hat{P}_8(M,1,+) = 1.133\ PI(M, m_\omega, m_{A_2}) + 0.476\ PI(M, m_\delta, m_{A_2})$$

$$+ 1.739\ PI(M, m_{A_2}, m_{A_2}) + 0.82\ PI(M, m_{\eta'}, m_B)$$

$$+ 1.259\ PI(M, m_{\eta'}, m_g) + 0.192\ PI(M, m_\delta, m_\delta)$$

$$+ 3.637\ PI(M, m_B, m_B) + 13.215\ PI(M, m_B, m_g)$$

$$+ 0.686\ PI(M, m_g, m_f) + 12.005\ PI(M, m_g, m_g)$$

$$+ 0.378\ PI(M, m_B, m_f)$$

$$\hat{P}_8(M,1,-) = 0.26\ PI(M, m_\eta, m_{A_2}) + 1.864\ PI(M, m_{\eta'}, m_{A_2})$$

$$+ 0.319\ PI(M, m_{\eta'}, m_\delta) + 1.672\ PI(M, m_\delta, m_B)$$

$$+ 0.087\ PI(M, m_\delta, m_f) + 3.038\ PI(M, m_\delta, m_g)$$

$$+ 1.503\ PI(M,m_B,m_{A_2}) + 0.071\ PI(M,m_f,m_{A_2})$$

$$+ 2.499\ PI(M,m_{A_2},m_g)$$

$$\Pi_9(M,0,+) = 0.108\ PI(M,m_{\eta'},m_{\eta'}) + 0.26\ PI(M,m_\delta,m_{A_2})$$

$$+ 0.059\ PI(M,m_{\eta'},m_f) + 0.214\ PI(M,m_{A_2},m_{A_2})$$

$$\Pi_9(M,0,-) = 1.133\ PI(M,m_B,m_{A_2}) + 2.058\ PI(M,m_{A_2},m_g)$$

$$\Pi_9(M,1,+) = 0.26\ PI(M,m_\delta,m_{A_2}) + 1.13\ PI(M,m_{\eta'},m_B)$$

$$+ 0.214\ PI(M,m_{A_2},m_{A_2}) + 2.053\ PI(M,m_{\eta'},m_g)$$

$$\Pi_9(M,1,-) = 0.322\ PI(M,m_{\eta'},m_{A_2}) + 0.26\ PI(M,m_{\eta'},m_\delta)$$

$$+ 1.133\ PI(M,m_B,m_{A_2}) + 0.082\ PI(M,m_f,m_{A_2})$$

$$+ 2.058\ PI(M,m_{A_2},m_g)$$

$$\Pi_{10}(M,0,+) = 0.088\ PI(M,m_{\eta'},m_{\eta'}) + 0.088\ PI(M,m_{A_2},m_{A_2})$$

$$\Pi_{10}(M,1,+) = 0.088\ PI(M,m_{A_2},m_{A_2})$$

$$\Pi_{10}(M,1,-) = 0.176\ PI(M,m_{\eta'},m_{A_2})$$

n=3

π/η π/ρ π/ω π/η' π/f

π/g

n=4

π/η η/η ρ/η ω/η η'/η

f/η g/η ρ/ρ ω/ρ η'/ρ

f/ρ g/ρ π/ω ω/ω η'/ω

f/ω g/ω π/η' f/η' g/η'

π/δ π/B π/A_2 f/f g/f

g/g

(*)

n=5

η/η	ρ/η	ω/η	η'/η	δ/η
B/η	A_2/η	f/η	g/η	ω/ρ
η'/ρ	δ/ρ	B/ρ	A_2/ρ	ω/ω
η'/ω	δ/ω	B/ω	A_2/ω	f/ω
g/ω	π/η'	δ/η'	B/η'	A_2/η'
f/η'	g/η'	π/δ	f/δ	g/δ
π/B	f/B	g/B	π/A_2	f/A_2
g/A_2	π/f	π/g		

n=6

η/η	ω/η	η'/η	δ/η	B/η
A_2/η	f/η	g/η	η'/ρ	δ/ρ
B/ρ	A_2/ρ	f/ρ	g/ρ	ω/ω
η'/ω	δ/ω	B/ω	A_2/ω	f/ω
g/ω	π/η'	η'/η'	δ/η'	B/η'
A_2/η'	f/η'	g/η'	δ/δ	B/δ
A_2/δ	f/δ	g/δ	B/B	A_2/B
f/B	g/B	π/A_2	A_2/A_2	f/A_2
g/A_2	f/f	g/f	g/g	

n=7

η'/η	δ/η	B/η	A_2/η	f/η
g/η	η'/ρ	A_2/ρ	η'/ω	δ/ω
B/ω	A_2/ω	f/ω	g/ω	η'/η'
δ/η'	B/η'	A_2/η'	f/η'	g/η'
δ/δ	B/δ	A_2/δ	f/δ	g/δ
B/B	A_2/B	f/B	g/B	A_2/A_2
f/A_2	g/A_2			

n=8

η'/η	A_2/η	η'/ω	A_2/ω	η'/η'
δ/η'	B/η'	A_2/η'	f/η'	g/η'
δ/δ	B/δ	A_2/δ	f/δ	g/δ
B/B	A_2/B	f/B	g/B	A_2/A_2
f/A_2	g/A_2	f/f	g/f	g/g

n=9

η'/η'	δ/η'	B/η'	A_2/η'	f/η'
g/η'	A_2/δ	A_2/B	A_2/A_2	f/A_2
g/A_2				

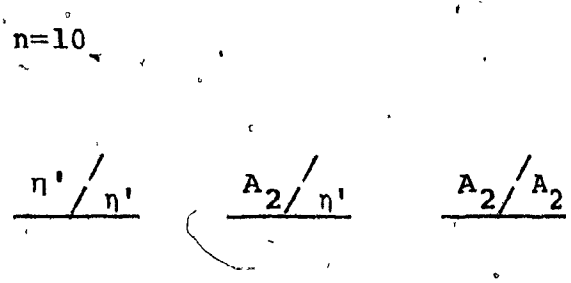

Figure A1: Schematic representation of initial conditions for equation (III.4.1). n is the number of pions emitted by the fireball.

APPENDIX II

Initial Conditions in the Linear Bootstrap (Exclusive Channels).

We state here the non-zero initial conditions used to evaluate exclusive channel probabilities in the linear bootstrap model (eq.III.5.1,III.5.2). They correspond to the diagrams of figure (A.2). The notation is the same as in appendix I. They are:

$$\hat{P}_3(M,1) = 1.5\ PI(M,m_\rho,m_\pi) + 4.05\ PI(M,m_f(f\to 2\pi),m_\pi) + 0.84\ PI(M,m_g(g\to 2\pi),m_\pi)$$

$$\hat{P}_4(M,0) = 1.182\ PI(M,m_{A_2},m_\pi) + 1.5\ PI(M,m_\rho,m_\rho) + 1.68\ PI(M,m_g(g\to 2\pi),m_\rho) + 8.201\ PI(M,m_f(f\to 2\pi),m_f(f\to 2\pi)) + 0.47\ PI(M,m_g(g\to 2\pi),m_g(g\to 2\pi))$$

$$\hat{P}_4(M,1) = 1.773\ PI(M,m_{A_2},m_\pi) + 12.15\ PI(M,m_f(f\to 2\pi),m_\rho) + 6.804\ PI(M,m_f(f\to 2\pi),m_g(g\to 2\pi))$$

$$\hat{P}_5(M,1) = 0.14\ PI(M,m_f,m_\pi) + 2.45\ PI(M,m_g,m_\pi) + 2.659\ PI(M,m_\rho,m_{A_2}) + 7.179\ PI(M,m_f,m_{A_2}) + 1.489\ PI(M,m_g,m_{A_2})$$

$$\hat{P}_6(M,O) = 4.9\ PI(M,m_g,m_\rho) + 2.744\ PI(M,m_g,m_g)$$

$$+ 1.047\ PI(M,m_{A_2},m_{A_2}) + 0.567\ PI(M,m_f,m_f)$$

$$\hat{P}_6(M,1) = 0.42\ PI(M,m_f,m_\rho) + 20.08\ PI(M,m_g,m_f)$$

$$+ 1.571\ PI(M,m_{A_2},m_{A_2})$$

$$\hat{P}_7(M,1) = 0.248\ PI(M,m_f,m_{A_2}) + 4.343\ PI(M,m_g,m_{A_2})$$

$$\hat{P}_8(M,O) = 0.01\ PI(M,m_f,m_f) + 4.002\ PI(M,m_g,m_g)$$

$$\hat{P}_8(M,1) = 0.686\ PI(M,m_f,m_g)$$

n=3

π/ρ π/f π/g

n=4

ρ/ρ f/ρ g/ρ π/A_2 f/f

g/f g/g

n=5

A_2/ρ π/f A_2/f π/g A_2/g

n=6

f/ρ g/ρ A_2/A_2 f/f g/f

g/g

n=7

f/A_2 g/A_2

n=8

f/f g/f g/g

Figure A2: Schematic representation of initial conditions for equations (III.5.1,III.5.2). n is the number of pions emitted by the fireball.

APPENDIX III

Initial Conditions in the Non-Linear Bootstrap(Exclusive Channels).

Non-zero initial conditions used to evaluate exclusive channel probabilities in the non-linear bootstrap model (eq. III.6.1,III.6.2) are stated here. These conditions which correspond to the diagrams of figure (A.3) must be added to the corresponding ones in appendix II. We denote by $I(M,m_1,m_2,m_3)$ the three-body phase-space (see appendix IV) and include in the coefficient all factors for identical particles. Thus, we have:

$$\overset{\gamma}{P}_4(M,O) = 0{,}5\ I(M,m_\pi,m_\pi,m_\rho) + 1.35\ I(M,m_\pi,m_\pi,m_f) + 0.28\ I(M,m_\pi,m_\pi,m_g)$$

$$\overset{\gamma}{P}_4(M,1) = 1.2\ I(M,m_\pi,m_\pi,m_\rho) + 2.025\ I(M,m_\pi,m_\pi,m_f) + 0.672\ I(M,m_\pi,m_\pi,m_g)$$

$$\overset{\gamma}{P}_5(M,1) = 1.064\ I(M,m_\pi,m_\pi,m_{A_2}) + 1.8\ I(M,m_\pi,m_\rho,m_\rho) + 2.016\ I(M,m_\pi,m_\rho,m_g) + 0.564\ I(M,m_\pi,m_g,m_g) + 8.2\ I(M,m_\pi,m_f,m_f) + 6.075\ I(M,m_\pi,m_\rho,m_f) + 3.402\ I(M,m_\pi,m_f,m_g)$$

$$P_6(M,O) = 0.047\ I(M,m_\pi,m_\pi,m_f) + 0.817\ I(M,m_\pi,m_\pi,m_g)$$

$$+ 1.773\, I(M,m_\pi,m_\rho,m_{A_2}) + 4.778\, I(M,m_\pi,m_f,m_{A_2})$$

$$+ 0.992\, I(M,m_\pi,m_g,m_{A_2}) + 6.075\, I(M,m_\rho,m_\rho,m_f)$$

$$+ 6.804\, I(M,m_\rho,m_f,m_g) + 11.072\, I(M,m_f,m_f,m_f)$$

$$+ 1.905\, I(M,m_f,m_g,m_g)$$

$$\rho_6(M,1) = 0.07\, I(M,m_\pi,m_\pi,m_f) + 1.96\, I(M,m_\pi,m_\pi,m_g)$$

$$+ 4.254\, I(M,m_\pi,m_\rho,m_{A_2}) + 7.179\, I(M,m_\pi,m_f,m_{A_2})$$

$$+ 2.382\, I(M,m_\pi,m_g,m_{A_2}) + 0.9\, I(M,m_\rho,m_\rho,m_\rho)$$

$$+ 4.536\, I(M,m_\rho,m_\rho,m_g) + 2.54\, I(M,m_\rho,m_g,m_g)$$

$$+ 0.474\, I(M,m_g,m_g,m_g) + 24.6\, I(M,m_\rho,m_f,m_f)$$

$$+ 13.778\, I(M,m_f,m_f,m_g)$$

$$\rho_7(M,1) = 5.88\, I(M,m_\pi,m_\rho,m_g) + 3.293\, I(M,m_\pi,m_g,m_g)$$

$$+ 0.567\, I(M,m_\pi,m_f,m_f) + 0.21\, I(M,m_\pi,m_\rho,m_f)$$

$$+ 10.04\, I(M,m_\pi,m_f,m_g) + 1.885\, I(M,m_\pi,m_{A_2},m_{A_2})$$

$$+ 3.191\, I(M,m_\rho,m_\rho,m_{A_2}) + 1.0\, I(M,m_g,m_g,m_{A_2})$$

$$+ 3.573\, I(M,m_\rho,m_g,m_{A_2}) + 15.188\, I(M,m_\rho,m_f,m_{A_2})$$

$$+ 6.03\, I(M,m_g,m_f,m_{A_2}) + 4.431\, I(M,m_f,m_f,m_{A_2})$$

Initial conditions contributing to the production of a higher

number of pions (n=8,9) are neglected.

n=4

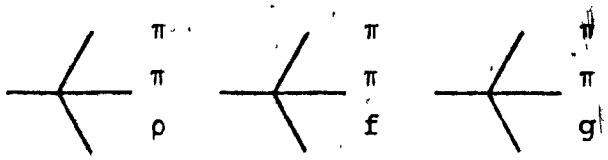
π π ρ
π π f
π π g

n=5

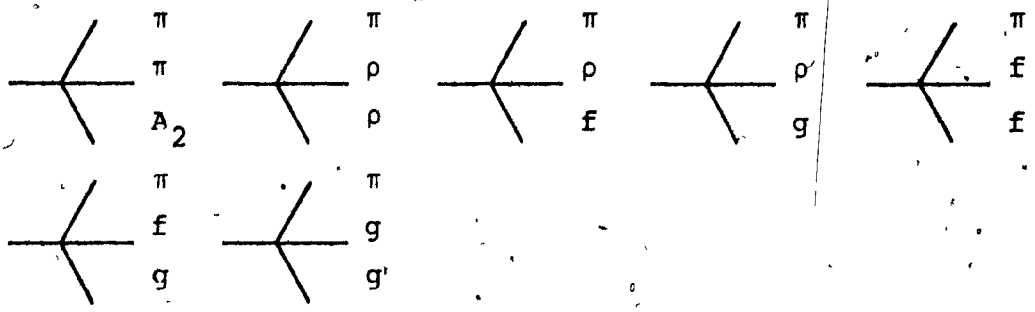
π π A2
π ρ ρ
π ρ f
π ρ g
π f f
π f g
π g g'

n=6

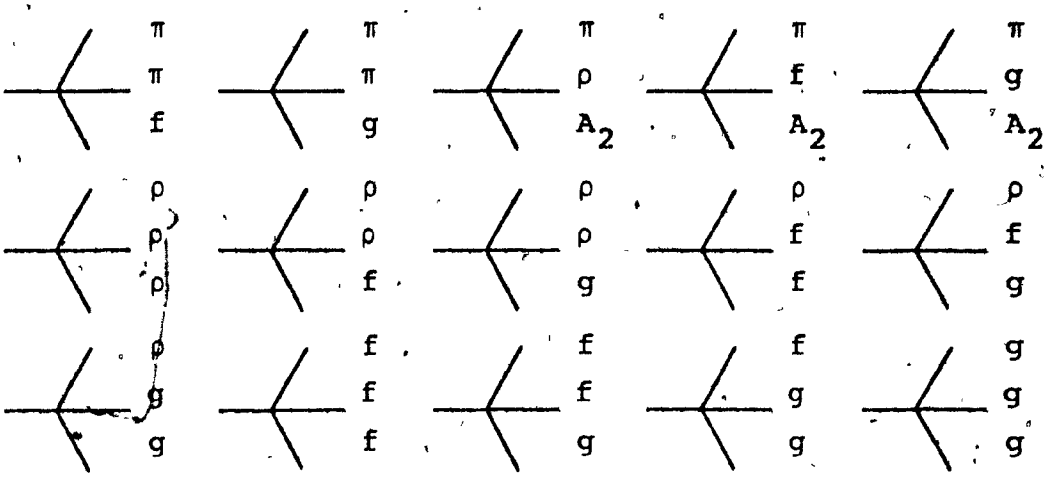
π π f
π π g
π ρ A2
π f A2
π g A2
ρ ρ ρ
ρ ρ f
ρ ρ g
ρ f f
ρ f g
ρ g g
f f f
f f g
f f g
g g g
g g g

n=7

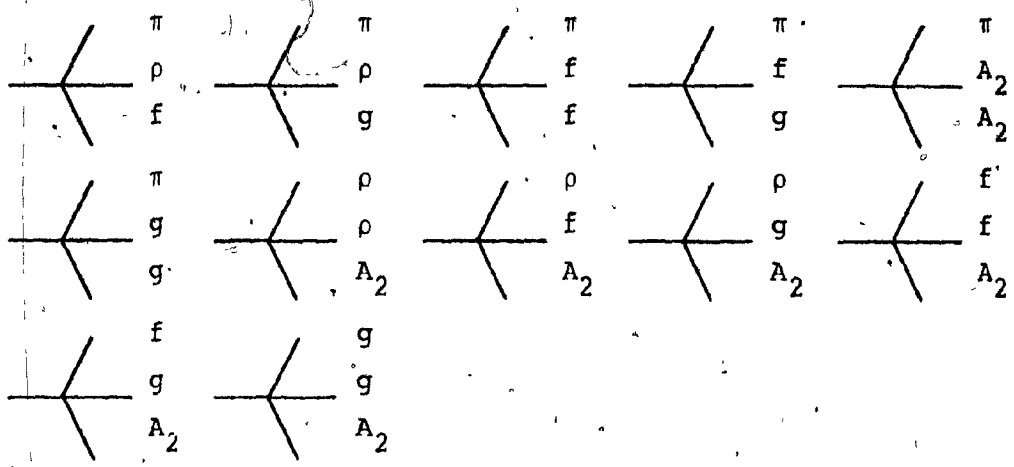

Figure A.3: Schematic representation of initial conditions for equations (III.6.1,III.6.2), non-linear terms only. n is the number of pions emitted by the fireball.

APPENDIX IV

Three-body Phase-space.

We shall here derive an exact expression for the non-invariant relativistic three-body phase-space where all three masses are different. In the center of mass of this system, the expression to calculate is the following:

$$I(M,m_1,m_2,m_3) = \int d^3p_1 d^3p_2 d^3p_3 \delta(\vec{p}_1+\vec{p}_2+\vec{p}_3)\,\delta(M-E_1-E_2-E_3) \times \theta(E_1)\,\theta(E_2)\,\theta(E_3) \qquad \text{(D-1)}$$

(The notation used is self-evident).

After integration over the two delta functions and using the identity:

$$dq_1 dq_2 d(\cos\theta) = \frac{E_1E_2E_3}{|\vec{q}_1|^2|\vec{q}_2|^2}\, dE_1 dE_2 dE_3 \qquad \text{(D-2)}$$

where θ is defined as the angle between $\vec{q}_1$ and $\vec{q}_2$, we obtain:

$$I(M,m_1,m_2,m_3) = 8\pi^2 \int dE_1 dE_2 E_1E_2\,(M-E_1-E_2)\,\theta(E_1)\,\theta(E_2)\,\theta(M-E_1-E_2) \times \theta\Big[4(E_1^2-m_1^2)(E_2^2-m_2^2) - \big[M^2-2M(E_1+E_2)+2E_1E_2-m_3^2$$

$$+m_1^2+m_2^2\Big]^2\Big] \qquad \text{(D-3)}$$

The last θ function comes from the momentum conservation requirement and defines the boundary of the integration region enclosed in. For instance, solving for E_1 gives:

$$\text{Lower limit:} \quad E_{1L} = \frac{b-\sqrt{d}}{2a}$$

$$\text{Upper limit:} \quad E_{1U} = \frac{b+\sqrt{d}}{2a} \qquad \text{(D-4)}$$

where

$$a \equiv (M^2-2ME_2+m_2^2)$$

$$b \equiv (M-E_2)(M^2-2ME_2+m_1^2+m_2^2-m_3^2)$$

$$d \equiv (E_2^2-m_2^2)\left[(M^2-2ME_2-m_1^2+m_2^2-m_3^2)^2-4m_1^2m_3^2\right]$$

Using these, the integral reduces to:

$$I(M,m_1,m_2,m_3) = \frac{2\pi^2}{3}\int_{E_{2L}}^{E_{2U}} dE_2 \left[(E_2^2-m_2^2)\left[(M^2-2ME_2-m_1^2+m_2^2-m_3^2)^2-4m_1^2m_3^2\right]\right]^{\frac{1}{2}}$$

$$\times \frac{E_2}{(M^2-2ME_2+m_2^2)^3}\left[3(M-E_2)^2\left[(M^2-2ME_2+m_2^2)^2-(m_1^2-m_3^2)^2\right]\right.$$

$$-(E_2^2-m_2^2)\left[(M^2-2ME_2-m_1^2+m_2^2-m_3^2)^2-4m_1^2m_3^2\right] \quad \text{(D-5)}$$

where the limits of integration are given by the zeros of the argument of the square root. They are:

$$E_{2L} = m_2$$

$$E_{2U} = \frac{1}{2M}\left[M^2+m_2^2-(m_1+m_3)^2\right] \quad \text{(D-6)}$$

This is our final answer. It is not possible to obtain a general fully integrated analytic result. Nevertheless, we can if two masses vanish. In this case, we have:

$$I(M,m,0,0) = \frac{\pi^2 M^5}{2.5!}\left[\left(1-\frac{m^2}{M^2}\right)\left(7-43\frac{m^2}{M^2}-23\frac{m^4}{M^4}-3\frac{m^6}{M^6}+2\frac{m^8}{M^8}\right)+120\frac{m^4}{M^4}\ln\left(\frac{M}{m}\right)\right] \quad \text{(D-7)}$$

When all masses vanish, this expression reduces to:

$$I(M,0,0,0) = \frac{7}{2}\frac{\pi^2}{5!}M^5 \quad \text{(D-8)}$$

These special cases were also obtained by Millburn (d.1).

REFERENCES

1.1 - E. Fermi, Prog. of Theor. Phys. 5,570,(1950).

1.2 - R. Hagedorn and J. Ranft, Nuovo Cimento Suppl. 6,169, (1968); Nucl. Phys. B47,157,(1972).

1.3 - F. Elvekjaer and F.Steiner, DESY preprint, DESY 76/15, (1976).

1.4 - W. Ernst et al., Bielefeld University preprint, BI-TP 78/05,(1978) and references therein.

1.5 - R.C. Hwa, Phys. Rev. Lett. 26,1143,(1971).

1.6 - G. Ranft and J. Ranft, Nucl. Phys. B69,285,(1974).

1.7 - For a review on diffraction phenomena in hadronic physics, see U. Amaldi, M. Jacob and G. Matthiae, Ann. Rev. Nucl. Sci.,385,(1976).

1.8 - M. Derrick et al.,Phys. Rev.D9,1853,(1974).

1.9 - F. C. Winkelmann et al., Phys. Rev. Lett. 32,121,(1974).

1.10 - T. J. Roberts et al., "Three-Pion Production on Complex Nuclei at 23 GeV/c", University of Illinois preprint; G. Ascoli et al., "Partial Wave Analysis of A_2 Production", University of Illinois preprint.

1.11 - V. Hungerbuehler et al., Phys. Rev. D10,2051,(1974).

1.12 - R. Gagnon and B. Margolis, "Statistical Description of Multipion Production in Diffractive Hadronic Reactions" Mc Gill University preprint, (in preparation).

1.13 - R. Hagedorn, Supp. al Nuovo Cimento 3,147,(1965).

1.14 - S. C. Frautschi, Phys. Rev. D3,2821,(1971).

1.15 - F. Johns, B. Margolis and W. J. Meggs, and R. K. Logan, Phys. Rev. Lett. 29,756,(1972).

1.16 - B. Margolis, W. J. Meggs and R. K. Logan, Phys. Rev. D8,199,(1973).

2.1 - C. J. Hamer, Nuovo Cimento 12A,162,(1972).

2.2 - M. Chaichian et al., Nucl. Phys. B92,445,(1975).

2.3 - E. Beth and G.E. Uhlenbeck, Physica 4,915,(1937).

2.4 - S.Z. Belenkij, Nucl. Phys. 2,259,(1956).

2.5 - C.J. Hamer and S.C. Frautschi, Phys. Rev. D4,2125,(1971).

2.6 - W. Nahm, Nucl. Phys. B45,525,(1972).

3.1 - A.H. Mueller, Phys. Rev. D2,2963,(1970).

3.2 - Chan Hong-Mo et al., Nucl. Phys. B54,411,(1973).

3.3 - D.P.Roy and R.G. Roberts, Nucl. Phys. B77,240,(1974).

3.4 - C.E. De Tar et al., Phys. Rev. Lett. 26,675,(1971).

3.5 - R.D. Field, G.C. Fox, Nucl. Phys. B80,367,(1974).

3.6 - B. Margolis, W.J. Meggs and N. Weiss, Phys. Rev. D13, 2551,(1976).

3.7 - E.L. Feinberg, Phys. Reports 5C,304,(1972).

3.8 - J.D. Jackson, Nuovo Cimento 34,1644,(1964).

3.9 - F. Selleri, Phys. Lett. 3,76,(1962).

3.10 - See for instance: B. Margolis, W.J. Meggs and S. Rudaz, Phys. Rev. D8,3944,(1973); B. Margolis and S.Rudaz, Phys. Rev. D9,653,(1974).

3.11 - R. Hagedorn, Nuovo Cimento 52A,1336,(1967).

3.12 - R. Harris, Thesis, University of Washington, VTL-PUB-22, p.273,(1975).

3.13 - J. Ballam et al., Phys. Rev D4,1946,(1971).

3.14 - For a recent review of the A_1 situation, see H.E. Haber and G.L. Kane, Nucl. Phys. B129,429,(1977).

3.15 - Yu. M. Antipov et al., Nucl. Phys. B63,141,153,(1973).

3.16 - B. Margolis and S. Rudaz, Phys. Rev. D9,653,(1974).

3.17 - First introduced by Drell and Hiida, Phys. Rev. Lett. 7,199,(1961).

3.18 - E.L. Berger, Phys. Rev. 166,1525,(1968); G. Ascoli et al., Phys. Rev. D9,1963,(1974).

3.19 - R.L. Schult and H.W. Wyld, Jr., Phys. Rev. D16,62,(1977).

3.20 - J. Pernegr et al., Nucl. Phys. B134,436,(1978).

3.21 - A. Ferrer et al., Phys. Lett. 74B,287,(1978).

3.22 - G. Alexander et al., Phys. Lett. 73B,99,(1978).

3.23 - G.L. Kane, The A_1 problem and should SU(3) multiplets be complete?, Proc. ANL Conf. on new directions in hadron spectroscopy, July 1975, ANL-HEP-CP-75-88.

4.1 - A. Fridman, Fortschr. Phys. 23,244,(1975); R. Harris, Thesis, University of Washington, VTL-PUB-22,p.10,(1975).

4.2 - K.Paler et al.,Phys. Rev. Lett. 26,1675,(1971).

4.3 - R. Harris et al., Phys. Lett. 59B,187,(1975); R. Harris et al., "Diffractive dissociation of pions in π d interactions at 15 GeV/c", Univ. of Washington preprint, VTL-PUB-43,(1977).

4.4 - R.J. Glauber, in "High Energy Physics and Nuclear Structure",edited by G. Alexander, North-Holland, Amsterdam, p.311,(1967); B. Margolis, Acta Phys. Pol. B2,57,(1971); K. Gottfried, Acta Phys. Pol. B3,769,(1972).

4.5 - U. Amaldi, M. Jacob and G. Matthiae, Ann. Rev. Nucl. Sci. 26,p.385,(1976); F. Bradamante et al., Phys. Lett. 31B, 87,(1970).

4.6 - B. Margolis and S. Rudaz, Phys. Rev. D9,653,(1974).

4.7 - Smaller than $A^2=4$ to account for shadowing effects.

4.8 - see ref. 12 in ref. 4.3b.

4.9 - Obviously these events will not necessarily disappear for internal dynamics may still play an observable role.

4.10 - Unless of course an extremely long run is performed.

5.1 - This conclusion was in fact drawn from the results obtained in pion-deuteron collision but since it does not depend on the target being a deuteron, we included it among those drawn from pion-proton scattering.

5.2 - R. Gagnon and B. Margolis, in preparation.

5.3 - Reported in A. Silverman, "Review of High Energy Photoproduction", "Proceedings of the 1975 International Symposium on Lepton and Photon Interactions at High Energies",p.355,(1975).

5.4 - Subject to modifications.

d.1 - R.H. Millburn, Rev. of Mod. Phys. 27,1,(1955).

PION-PROTON SCATTERING AT LARGE S VALUES.

NUMBER OF EVENTS*

	FULL CALCULATION		VERTICES: π/F INIT.COND: π/K	VERTICES: π/F INIT.COND: π/ρ, $\pi/f \to 2\pi$, $\pi/g \to 2\pi$
	Linear	Non-Linear	Linear	Linear
3π	303.8	303.8	303.8	303.8
5π	40.14	40.75	23.38	15.32
7π	4.99	5.15	1.30	.86
9π	$\sim$0.66	$\sim$.68	$\sim 8.6 \times 10^{-2}$	$\sim 5.1 \times 10^{-2}$
$\sigma(3\pi)/\sigma(5\pi)$	7.57	7.46	12.99	19.83
$\sigma(3\pi)/\sigma(7\pi)$	60.9	59.0	234	353
$\sigma(3\pi)/\sigma(9\pi)$	$\sim$460	$\sim$ 447	$\sim$3533	$\sim$5957

* Overall arbitrary normalization

Table I

PION-DEUTERON SCATTERING AT P_{LAB}=15 GeV/c

NUMBER OF EVENTS*

	FULL CALCULATION				VERTICES: π/F INIT.COND: π/R		VERTICES: π/F INIT.COND: π/ρ π/f→2π, π/g→2π	
	Linear		Non-linear		Linear		Linear	
	b=31	b=33.67	b=31	b=33.67	b=31	b=33.67	b=31	b=33.67
3π	944.3	933.5	944.3	933.5	944.3	933.5	944.3	933.5
5π	54.94	51.52	55.73	52.24	35.35	33.38	20.36	19.10
7π	.842	.707	.867	.727	.309	.265	.163	.139
9π	3.35×10^{-3}	2.41×10^{-3}	3.50×10^{-3}	2.47×10^{-3}	8.58×10^{-4}	6.43×10^{-4}	4.47×10^{-4}	3.35×10^{-4}
σ(3π)/σ(5π)	17.19	18.12	16.94	17.87	26.71	27.97	46.38	48.87
σ(3π)/σ(7π)	1121	1320	1089	1284	3056	3523	5793	6716
σ(3π)/σ(9π)	2.82×10^{5}	3.87×10^{5}	2.70×10^{5}	3.78×10^{5}	1.10×10^{6}	1.45×10^{6}	2.11×10^{6}	2.79×10^{6}

* Normalization to hydrogen is provided by equation (IV.2.5) with $(\sigma^{T}_{\pi D}/\sigma^{T}_{\pi p})^{2}=3.6$

Table II

FIGURE CAPTIONS

Figure I: ln $\{M^3\rho(M)\}$ versus M. $\rho(M)$ is the total density of states we have calculated for different isospin, G-parity combinations.

(upper full curve) : $I^G=1^-$

(lower full curve) : $I^G=0^-$

(- - -) : $I^G=1^+$

(-·-·-·) : $I^G=0^+$

(— — —) : continuation of the I=1 curves

Figure II: Three-pion mass distribution in pion-proton scattering: A_1 and A_3 regions.

Figure III: Three-pion mass distribution in pion-proton scattering: A_1 region. Data from reference 3.13.

Figure IV: Five-pion mass distribution in pion-proton scattering.

(————) : full spectrum

(- - - -) : vertices πF
initial conditions πR

(.....) : vertices πF
initial conditions $\pi\rho$, πf, πg

Figure V: Five-pion mass distribution in pion-proton scattering (full spectrum).

(———) : with the analytic asymptotic density of states

(- - -) : with the calculated density of states

Figure VI: Seven-pion mass distribution in pion-proton scattering

(———) : full spectrum

(- - -) : vertices πF
initial conditions πR

(.....) : vertices πF
initial conditions $\pi\rho$, πf, πg

Figure VII: Nine-pion mass distribution in pion-proton scattering

(———) : full spectrum

(- - -) : vertices πF
initial conditions πR

(.....) : vertices πF
initial conditions $\pi\rho$, πf, πg

Figure VIII: Three-pion mass distribution in pion-deuteron scattering (p_{Lab}=15 GeV/c). Data from reference 4.3.

Figure IX: Five-pion mass distribution in pion-deuteron scattering (p_{Lab}=15 GeV/c). Data from reference 4.3.

Figure X: Seven-pion mass distribution in pion-deuteron scattering (p_{Lab}=15 GeV/c).

Figure XI: Nine-pion mass distribution in pion-deuteron scattering (p_{Lab}=15 GeV/c).

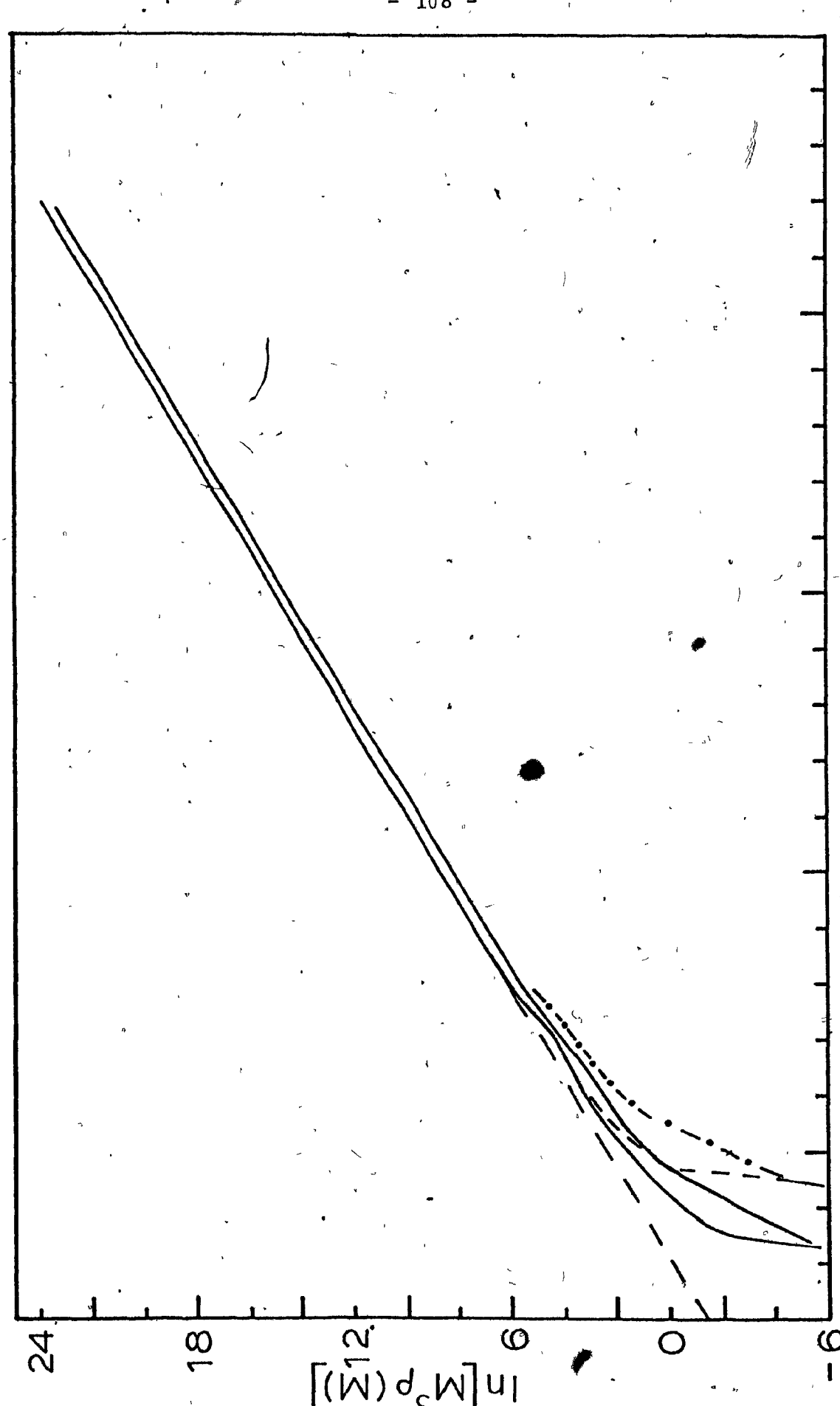

Figure 1.

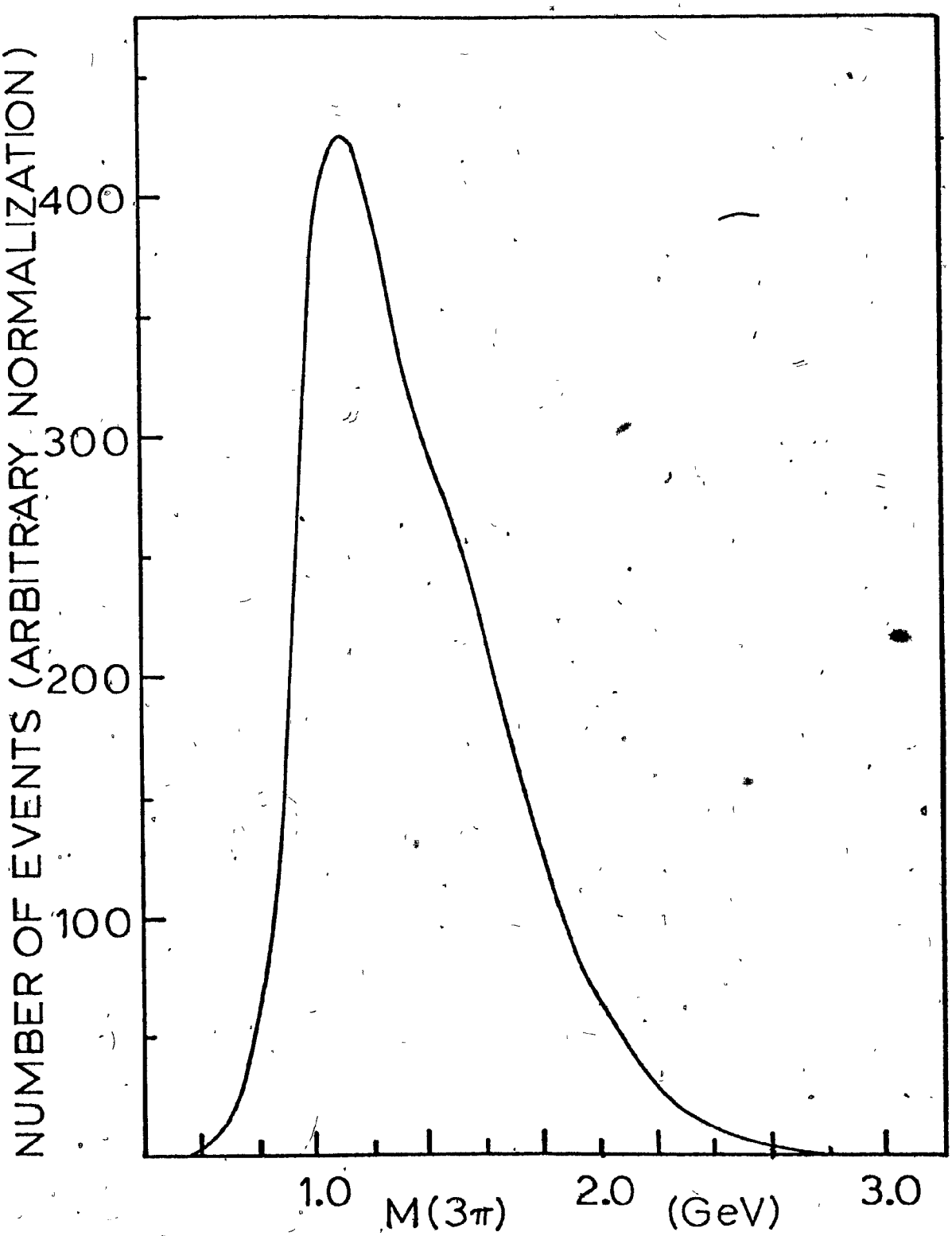
NUMBER OF EVENTS (ARBITRARY NORMALIZATION)
400
300
200
100
1.0
M(3π)
2.0
(GeV)
3.0

Figure 2.

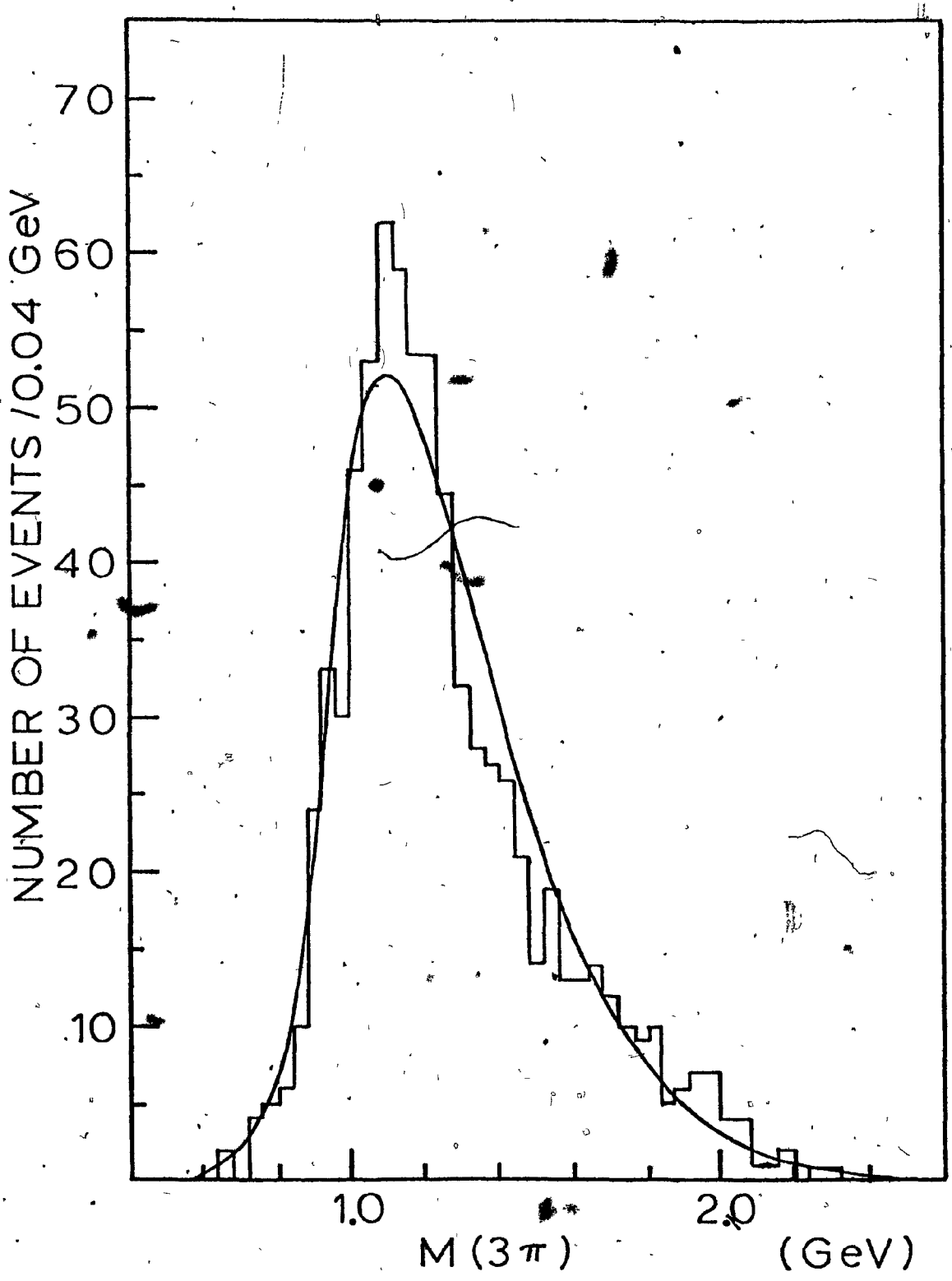

Figure 3.

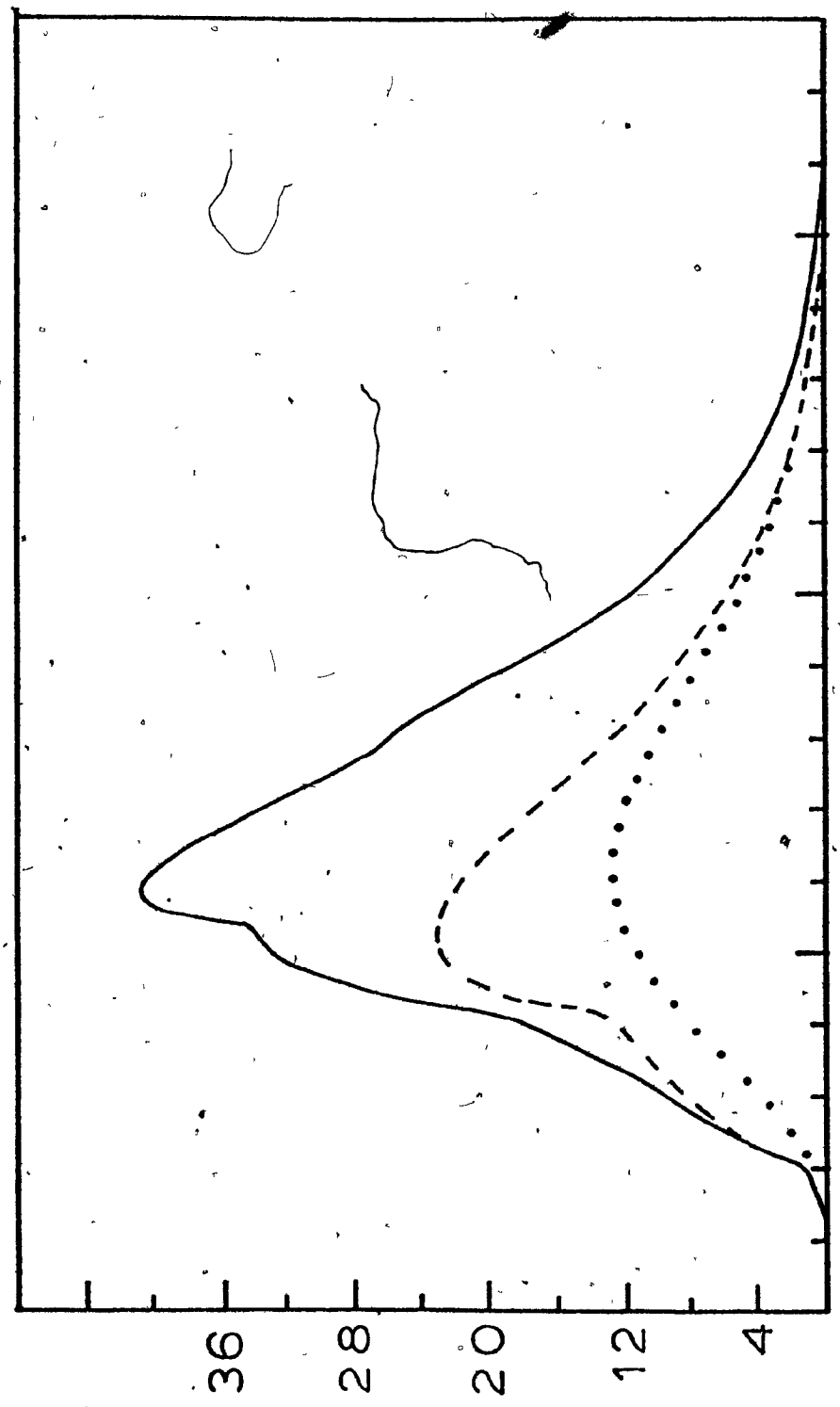
NUMBER OF EVENTS
(ARBITRARY NORMALIZATION)
36
28
20
12
4
1.0
2.0
3.0
4.0
M(5π) (GeV)

Figure 4.

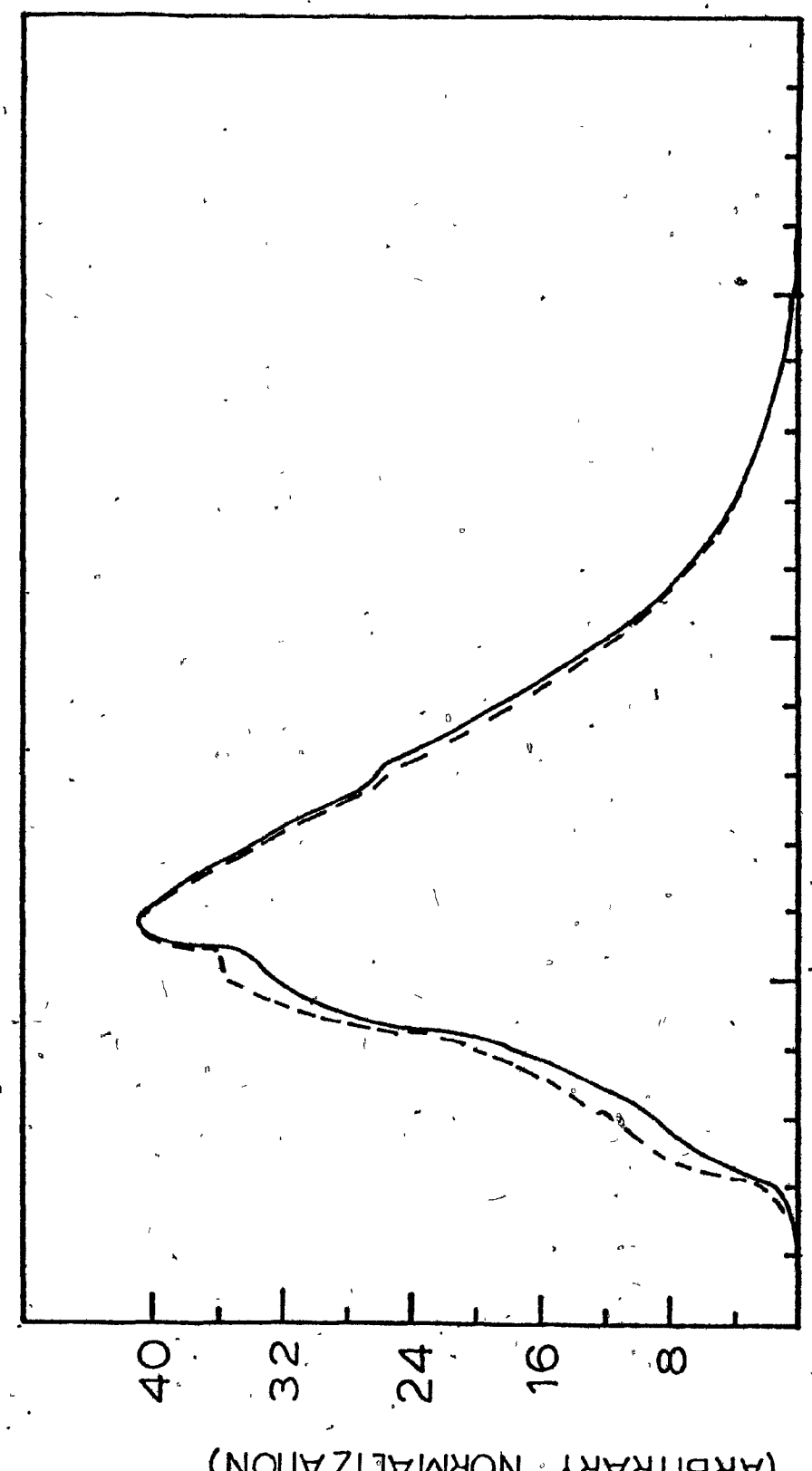
NUMBER OF EVENTS
(ARBITRARY NORMALIZATION)
40
32
24
16
8
1.0
2.0
3.0
4.0
M(5π) (GeV)

Figure 5.1

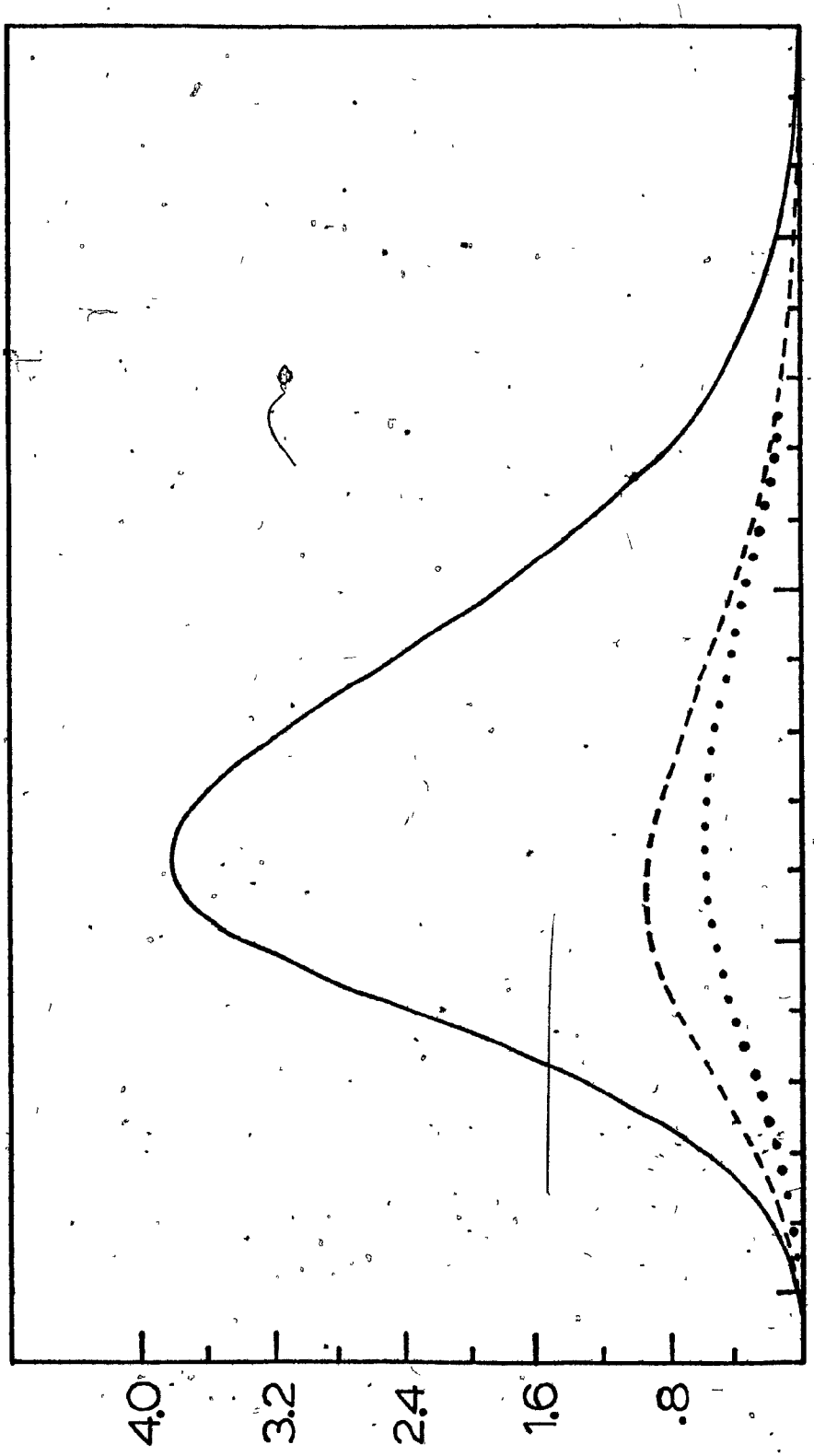
NUMBER OF EVENTS
(ARBITRARY NORMALIZATION)
4.0
3.2
2.4
1.6
.8
2.0
3.0
4.0
5.0
M(7π)
(GeV)

Figure 6.

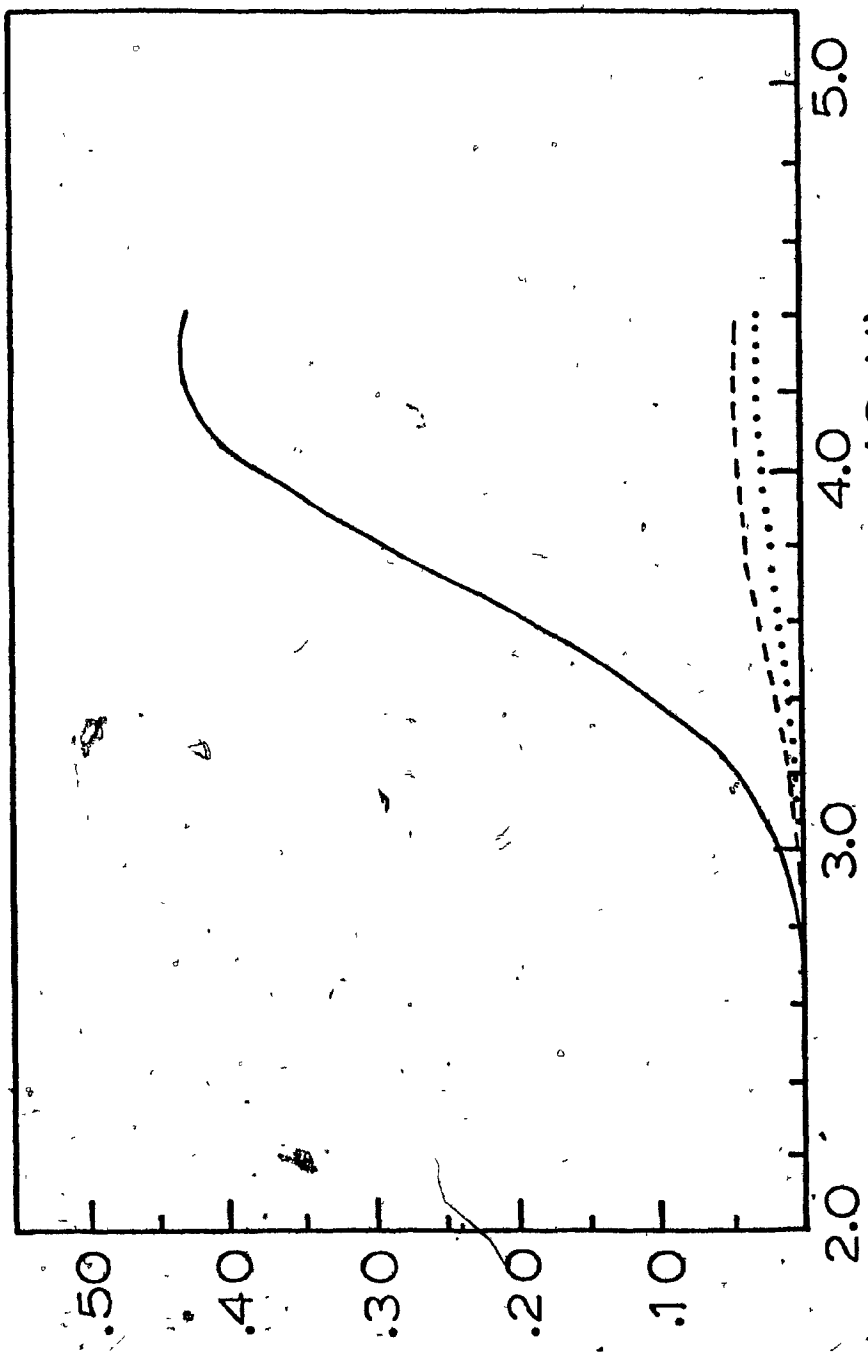
NUMBER OF EVENTS
(ARBITRARY NORMALIZATION)
.50
.40
.30
.20
.10
2.0
3.0
4.0
5.0
M(9π)
(GeV)

Figure 7.

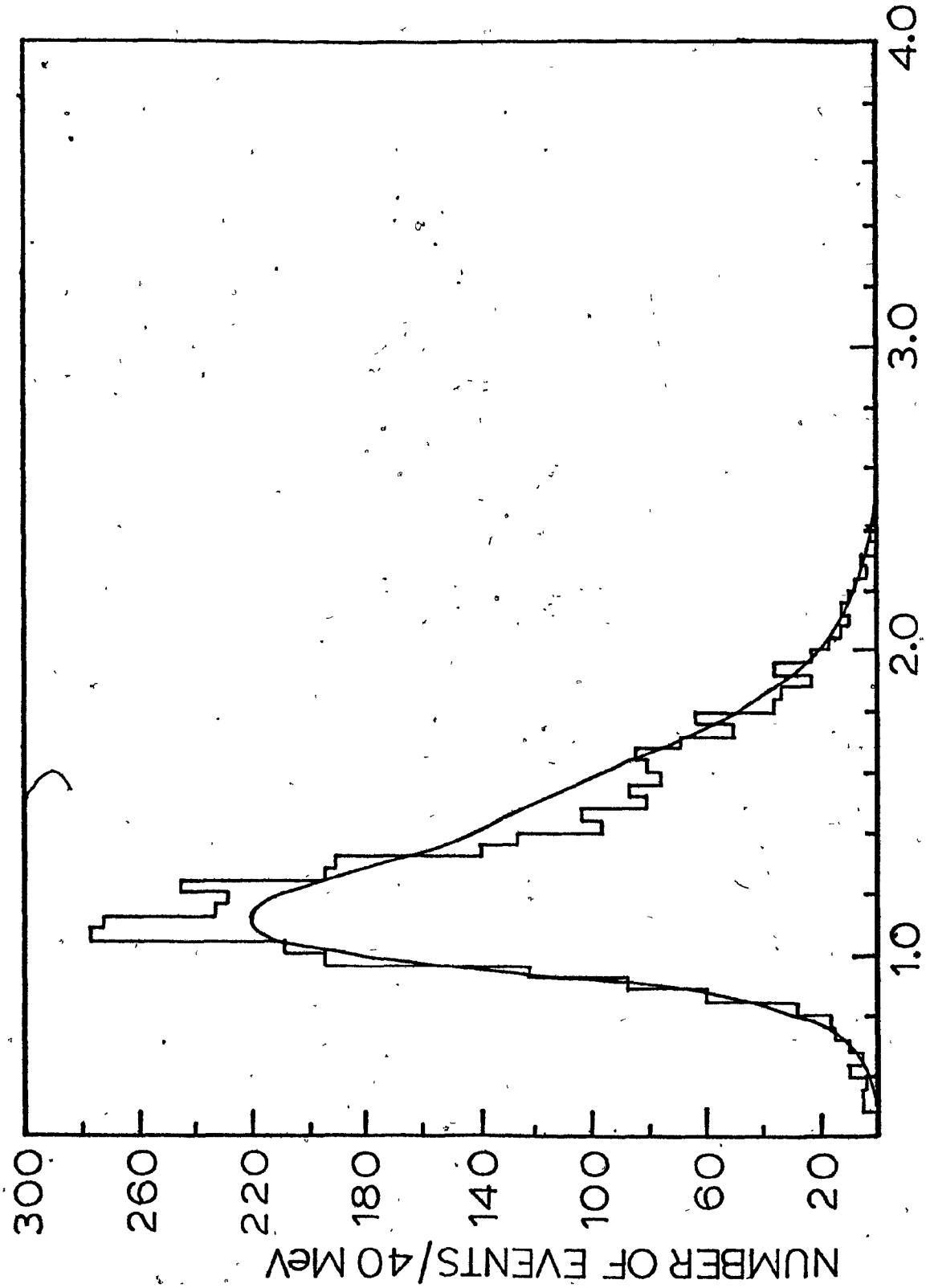
NUMBER OF EVENTS/40 MeV
300
260
220
180
140
100
60
20
1.0
2.0
3.0
4.0
M(3π)
(GeV)

Figure 8.

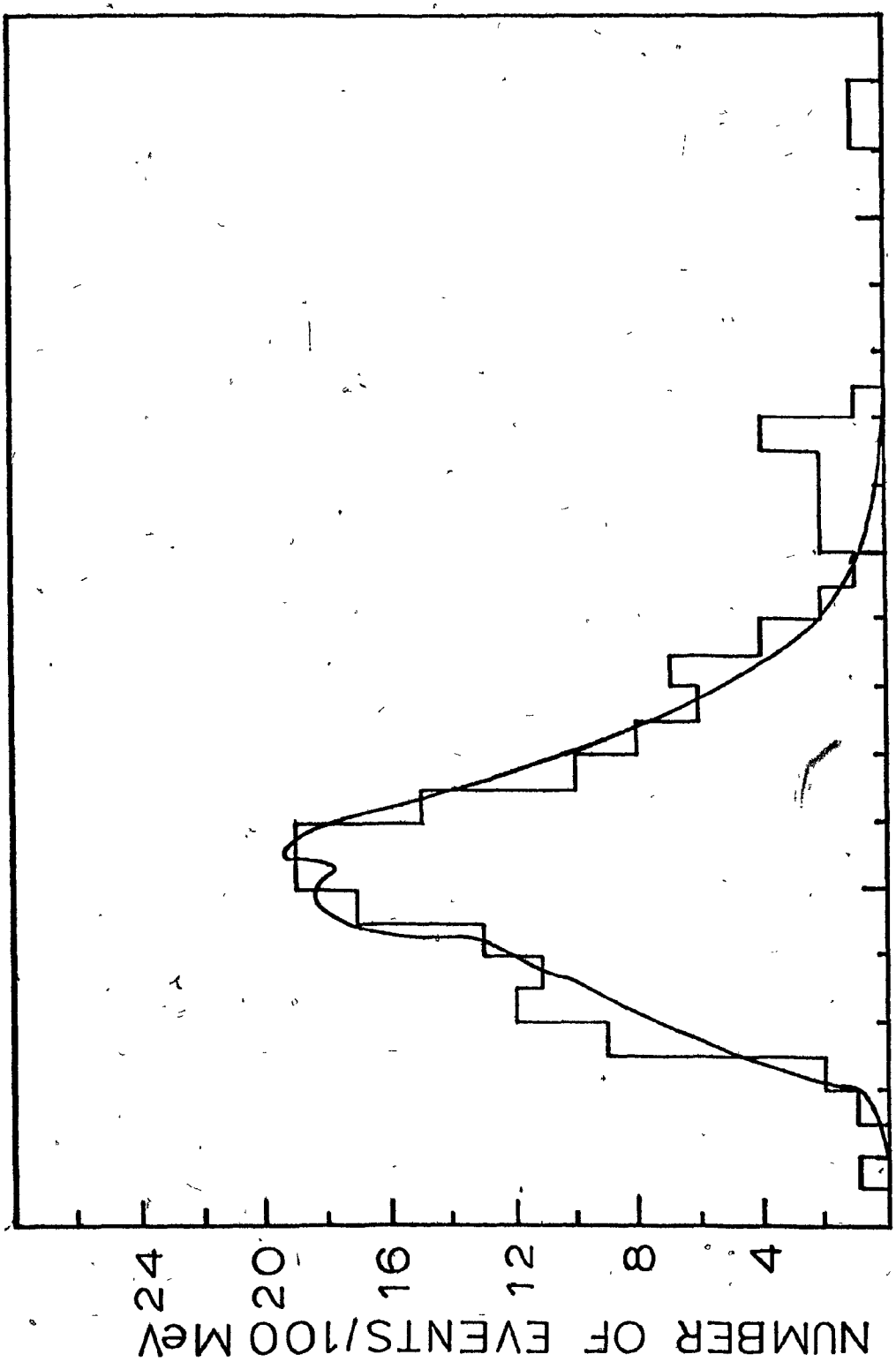

Figure 9:

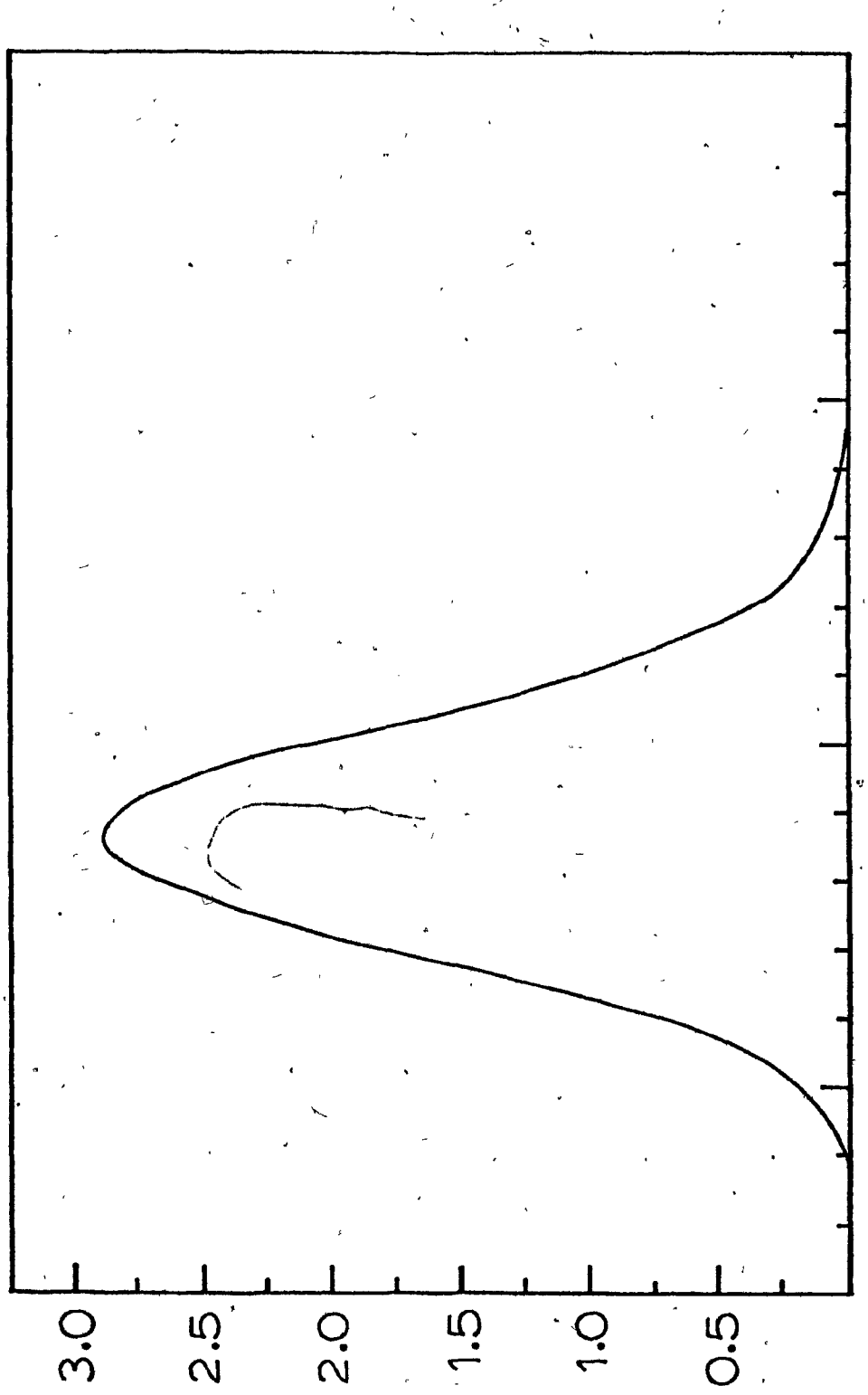
NUMBER OF EVENTS
(ARBITRARY NORMALIZATION)
3.0
2.5
2.0
1.5
1.0
0.5
2.0
3.0
4.0
5.0
M(7π)
(GeV)

Figure 10.

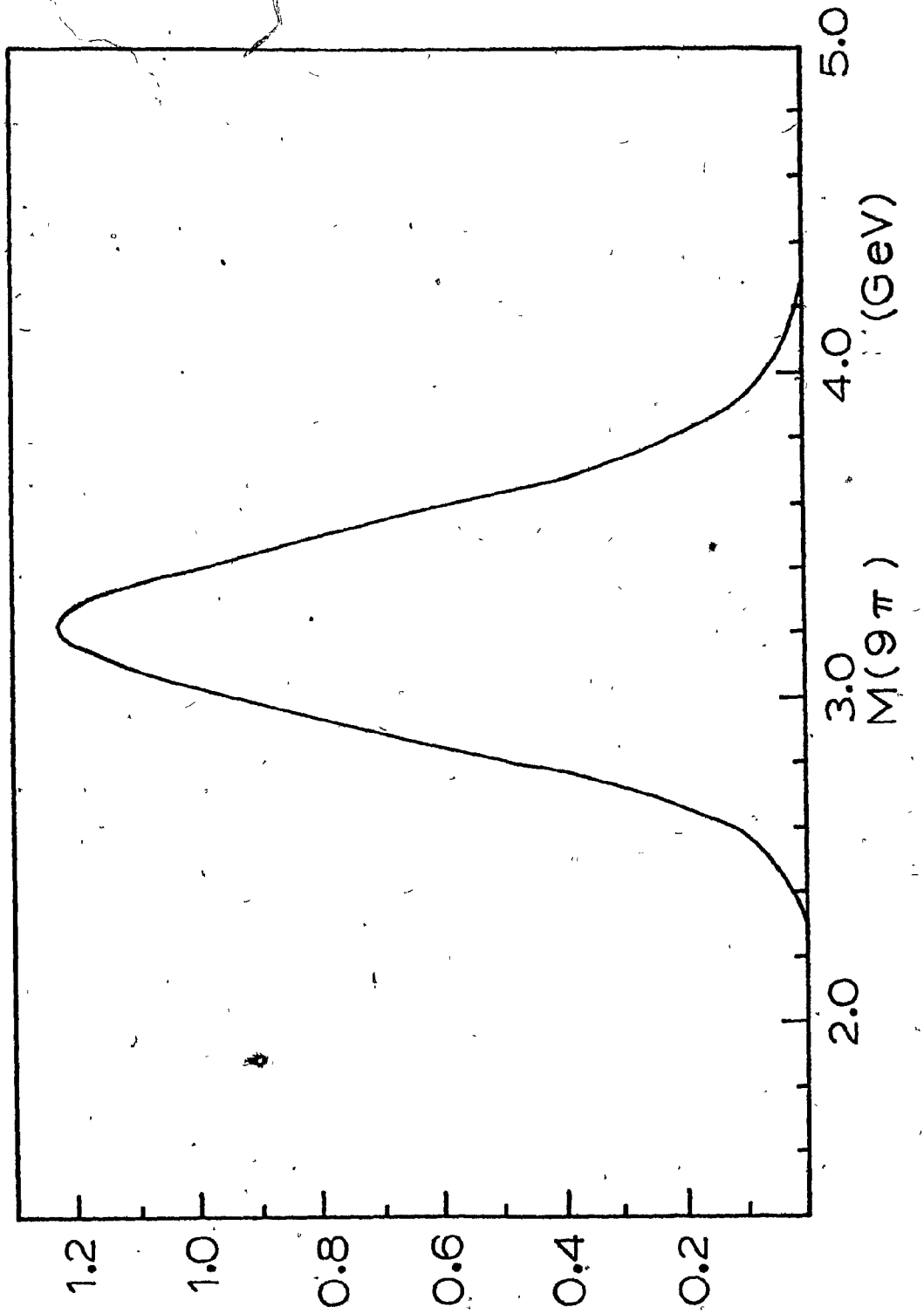
NUMBER OF EVENTS
(ARBITRARY NORMALIZATION)
1.2
1.0
0.8
0.6
0.4
0.2
2.0
3.0
4.0
5.0
M(9π) (GeV)

Figure 11.